Engineering Proteins via Peptide Backbone Mutagenesis: The Effects of Thioamide Linkages on the Folding and Stability of Short Peptides

Author: Kristen Ann Demick

Boston College

The Graduate School of Arts and Sciences

Department of Chemistry

ENGINEERING PROTEINS VIA PEPTIDE BACKBONE MUTAGENESIS: THE EFFECTS OF THIOAMIDE LINKAGES ON THE FOLDING AND STABILITY OF SHORT PEPTIDES

a thesis

by

KRISTEN ANN DEMICK

submitted in partial fulfillment of the requirements

for the degree of

Master of Science

August 2009

Engineering Proteins via Peptide Backbone Mutagenesis: The Effects of Thioamide Linkages on the Folding and Stability of Short Peptides

By: Kristen A. Demick

Advisor: Jianmin Gao

Abstract

The development of proteins/peptides as therapeutic agents has emerged as a promising area for drug design. Due to increased antibiotic resistance, search for novel antibiotics has become a primary area of interest within the pharmaceutical industry. Antimicrobial peptides have been a significantly desirable model due to their innate cytolytic effects and favorable interaction with the membranes of bacterial cells within the host. Thioxylated analogues of biologically active peptides have shown increased enzymatic stability and increased selectivity and potency. Thioamide linkages have thus been installed in a variety of short peptides, replacing the backbone amide linkage, in order to study the effects on peptide conformation and stability. Several bioanalytical tools were used in the analysis including circular dichroism spectroscopy, NMR, size-exclusion high performance liquid chromatography, and fluorescence. The mutation was well-accommodated within several systems, including Trpzip 4 and gramicidin A, and proved to have comparable, and in several cases, enhanced stability in comparison to the wild-type peptides.

Index of Abbreviations

AMP	Antimicrobial peptide
CD	Circular dichroism
DCM	Dichloromethane
DMF	Dimethylformamide
DMSO	Dimethylsulfoxide
DOPC	1,2-dioleoyl-*sn*-glycero-3-phosphocholine
Et_2O	Diethyl ether
EtOAc	Ethyl acetate
F2*F-MW-β-hairpin	MW-β-hairpin Phe^2 thioamide mutant
F12*Fgb1	gb1 Phe^{12} thioamide mutant
Fmoc	Fluorenylmethyloxycarbonyl
gA	Gramicidin A
M	Molar
MeCN	Acetonitrile
MeOH	Methanol
MW-β-hairpin	Ac-RFVOVNGKEIFQ-NH_2
Na_2SO_4	Sodium sulfate
NaOH	Sodium hydroxide
NH_4Cl	Ammonium chloride solution
P_4S_{10}	Phosphorus pentasulfide
Phe	Phenylalanine
RP-HPLC	Reverse-phase high performance liquid chromatography

SEC-HPLC	Size-exclusion high performance liquid chromatography
SPPS	Solid-phase peptide synthesis
TFE	Trifluoroethanol
THF	Tetrahydrofuran
Trp	Tryptophan
UV/Vis	Ultraviolet/visible light spectroscopy
W5*W-Trpzip 4	Trpzip 4 Trp^{5} thioamide mutant
WTgA	Wild-type gramicidin A
W9,11FgA	Gramicidin A double phenylalanine mutant
W9,11FgAT10	Gramicidin A D-Leu^{10} thioamide mutant
W9,11FgAT12	Gramicidin A D-Leu^{12} thioamide mutant

Table of Contents

Acknowledgements

I would like first to address my advisor, Professor Jianmin Gao, for financial and academic support. From the moment I met you, I could tell how excited you were about the research you planned to start at Boston College as a first-year professor. Your enthusiasm was contagious, and I knew instantly I wanted to help start this new group. I would like to thank you not only for your guidance and wisdom in the laboratory, but also for your willingness to support the decision I made to pursue a career outside of the lab where we both knew I was destined to be. I would also like to thank the Gao Group members. Though we were a brand new lab, we all stuck together to build a productive and positive learning environment. Thank you for everything throughout the last two years.

Special thanks to Grace Bauer and Christopher Pace. You both have become great friends over this past year and provided me with optimism vital to my success. I can't forget my McLaughlin Group boys: Joseph Arico, Eric Hardter, Nick Greco, and Christopher Theile. You've all made my time at Boston College a truly memorable experience.

Next, I would like to thank Dale Mahoney for her support and open ears. You helped make this a smooth transition. Thank you to John Boylan for all of your help both in and out of the NMR room. Additional thanks to Professor Udayan Mohanty for being a great role model in the classroom.

I'd finally like to take the time to express my sincerest gratitude to my parents who have been nothing but supportive of every decision I've made. Thank you for your encouragement and patience through this crazy journey. Crystal and Katie, thank you for

tolerating me during my first crazy year of graduate school, and last but not least, Lydia. You've been everything I've needed and more, and I couldn't have done this without you…*Go Eagles*!

CHAPTER 1

Introduction

1.1 Proteins/Peptides as Therapeutic Agents

1.1.1 Overview

As one of the most studied fields in modern chemical biology, the possibilities in using proteins as therapeutics seem endless. Their advantages must be exploited to their highest capacity. As biological entities, proteins are usually highly specific, which is a very desirable feature as a therapeutic agent. There are currently more than 130 proteins or peptides approved for clinical use by the FDA, and many more follow closely in development.[1]

There are a variety of uses for protein therapeutics. First, there are a wide range of vaccines; for example, the hepatitis B vaccine. This was created by producing recombinant hepatitis B surface antigen (HBsAg) protein. Significant immunity to the hepatitis B virus results when a patient is treated with this protein. There are also a group of enzymes and regulatory proteins that serve as therapeutics. These are introduced into the body in the event of a protein deficiency or abnormal protein production. One example is providing lactase to patients lacking that gastrointestinal enzyme or replacing vital blood-clotting factors (factor VIII and IX) in haemophiliacs. A third group of therapeutics uses antigen recognition sites of immunoglobulin (Ig) molecules or the receptor-binding domains of native protein ligands to direct the immune system to destroy particularly targeted cells. Several of these proteins have been approved for the treatment of inflammatory diseases.[1]

Diabetes, a common metabolism disorder, is a condition characterized by high blood glucose levels (hyperglycemia) brought on by defects in insulin secretion or insulin

action in the body. Insulin, a peptide hormone produced in the pancreas, is responsible for many metabolic functions and causes cells in the liver, muscle, and fat tissue to take up glucose from the blood. The body then stores the glucose as glycogen, a usable energy source. Insulin delivery can thus be a simple treatment to diabetes. Insulin is stored in the body as a hexamer, however, the active form is monomeric (Figure 1.1).[2]

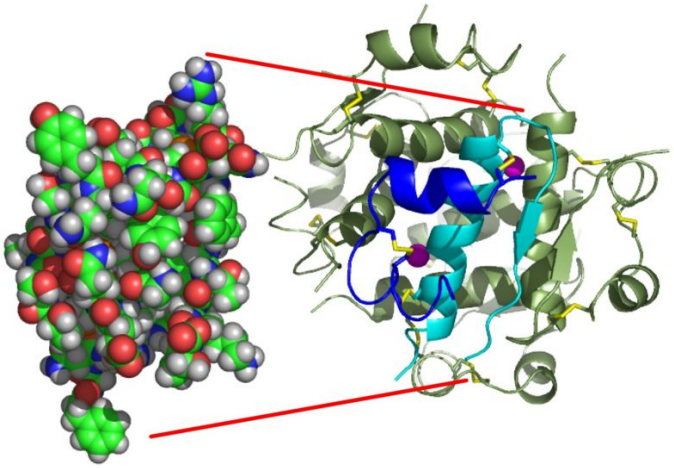

Figure 1.1: The structure of insulin. Space-filling model of the insulin monomer, believed to be biologically active (left). Carbon-green, hydrogen-white, oxygen-red, and nitrogen-blue. Right: insulin hexamer; A monomer unit is highlighted with the A chain in blue and the B chain in cyan. Yellow denotes disulfide bonds, and magenta spheres are zinc ions. Figure adapted from Reference 2.

Some of the most prominent diseases in the present culture seem to be increasing in fatality rates. Peptide drug design has been making dramatic strides to solve these problems. For example, Enfuvirtide, commonly known as Fuzeon, is a chemically

synthesized peptide serving as a fusion inhibitor of the HIV-1 virus from host T-cells. This moderately new drug, approved by the FDA in March of 2003, is a linear 36-amino acid peptide composed of naturally occuring L-amino acid residues: CH_3CO-Tyr-Thr-Ser-Leu-Ile-His-Ser-Leu-Ile-Glu-Glu-Ser-Gln-Asn-Gln-Gln-Glu-Lys-Asn-Glu-Gln-Glu-Leu-Leu-Glu-Leu-Asp-Lys-Trp-Ala-Ser-Leu-Trp-Asn-Trp-Phe-NH_2. Fuzeon disrupts the final stage of fusion of the HIV-1 virus with the target cell, preventing uninfected cells from becoming infected. It binds to the host CD4+ cell receptor via a viral transmembrane protein GP41 preventing the conformational change necessary for the fusion of the viral membrane to the host cell membrane. Fusion (or entry) inhibitors are a new class of antiretroviral drugs,[2] but are just one example of peptides serving as therapeutic agents.

The promising development of these protein and peptide drugs leads to all the possible types of proteins that could be used as therapeutic agents. It is necessary, though, to better understand the structural requirements and metabolic stability, as well as mechanistic action in the host, in order to best advance the field.

1.1.2 Antimicrobial Peptides

One of the most promising areas for peptides as therapeutics are antimicrobial peptides. Antimicrobial peptides (AMPs) have been isolated from a variety of species, including bacteria, fungi, plant and animal life. In fact, most living organisms rely on AMPs as a crucial component of their natural defense system. They are responsible for the direct killing and immunomodulatory effects in host defense against pathogenic

organisms. AMPs exhibit activity against Gram-positive and –negative bacteria, yeasts, and fungi, as well as possessing antiviral and anticancer properties.[3]

AMPs, also referred to as host-defense peptides, have a great diversity in their primary structure, however, the vast majority are relatively short and characterized by a predominance of cationic and hydrophobic amino acids. They differ in both secondary and tertiary structures, but are typically amphipathic in nature, containing both a hydrophilic and hydrophobic surface. This feature plays an important role in their antimicrobial mechanisms.[4] The hydrophobicity allows for enhanced interaction with lipid bilayers, whereas its hydrophilic surface allows for favorable interactions with the surrounding aqueous environment.

There are several classes of antimicrobial peptides. The most common are the linear cationic α-helical peptides, containing less than 40 amino acids. This class lacks cysteine residues and sometimes has a hinge or “kink” region in the middle of the peptide. Although in aqueous solutions these peptides are disordered, they convert to an α-helix in the presence of sodium dodecylsulphate micelles and phospholipid vesicles. The extent of α-helicity directly correlates to the antibacterial activity. Examples of peptides in this class are cecropins from insects and nematodes and LL36 from humans.[5]

Other classes of AMPs have secondary structures such as β-sheet structures, however, these AMPs are generally less active than the well-defined α-helical peptides. There exist anionic and cationic peptides containing multiple cysteine residues that allow disulfide bond formation, inducing stable β-sheet character. These peptides form a diverse family of defensins. An example of a β-defensin (3 disulfide bonds) is HBD1 in

humans. There are also α-defensins comprised of four intramolecular disulfide bonds, for instance HNP-1 and -2 in humans.[5]

Since the activity of AMPs is governed by factors such as conformation and structure, charge, size, and hydrophobicity, these factors must all be considered in drug development. Chemical synthesis of these peptides or analog peptidomimetics that will treat bacterial infections is desirable[3] and could make a large impact on modern medicine. Because antibacterial resistance has increased dramatically, the demand for new antibiotics is very high, and because of the structural diversity and biological compatibility of peptides, they serve as a great target for a new class of drugs. Though there exists a broad range of natural AMPs isolated in humans, they are still mechanistically puzzling.

1.1.3 Peptide-Membrane Interactions

Disruption of bacterial membranes is believed to be the mechanism of the antimicrobial action of AMPs. Mechanistic studies within model systems are thus necessary to see how these peptides are actually accomplishing membrane penetration. Membranes differ significantly with respect to their composition of lipids. This directly reflects the functional specialization of each particular membrane. In general, however, membranes contain proteins serving as transporters or enzymes covalently linked either directly to the lipids or to complex arrays of carbohydrates. Because the phospholipid bilayer is impermeable to polar compounds and charged solutes, often other factors are necessary for protein insertion. Nonpolar compounds, however, are most easily incorporated into membranes due to the thermodynamic driving force, hydrophobicity.

Fatty acyl groups of lipid tails accommodate the hydrophobic regions of amino acids, providing a close association with the membrane. This anchor cannot be perturbed without harsh denaturation conditions or other means that would interfere with the hydrophobics of the system. These proteins are referred to as integral membrane proteins. They differ from peripheral membrane proteins whose association with a membrane is governed by electrostatics and hydrogen bonding (and limited hydrophobic interactions) and can be released by a simple change of pH or ionic strength. Integral membrane proteins make up approximately 30% of all proteins, true for many species. [6]

Extensive research is being done within a variety of model systems in order to provide insight into other similar systems as to how these proteins interact with cell membranes. Cytolytic effects are believed to be a result of the peptide's interaction with membranes. Furthermore, once the mechanism of attack is understood, peptide engineering will quickly advance and synthetic analogues can be prepared and used as therapeutic agents.[7]

Several postulates have been made as to the mechanism of the antimicrobial-peptide-induced killing of bacterial cells (Figure 1.2). First is the barrel-stave model. Here, the attached peptides aggregate on the surface of the membrane and insert into the bilayer so that the hydrophobic regions of the peptide align with the lipid core region, allowing for the hydrophilic regions to form the interior region of the pore. Next is the carpet model which is, again, initiated by the aggregation of the peptides on the membrane surface. The membrane is then disrupted because the peptides orient parallel to the surface of the lipid bilayer and form an extensive layer ("carpet"). Finally, in the toroidal model, the attached peptides aggregate and induce the lipid monolayers to bend

continuously through the pore so that the water core is lined by both the inserted peptides and the lipid head groups.[5]

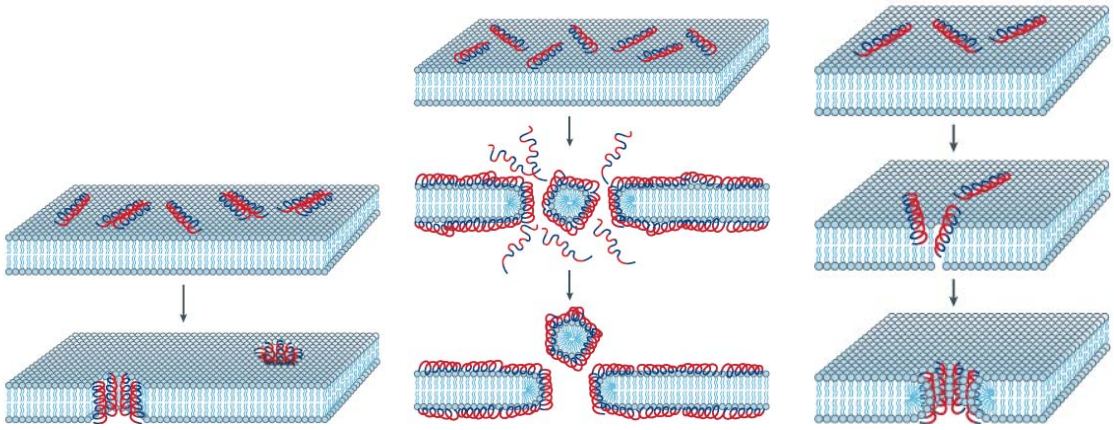

Figure 1.2: Models of antimicrobial-peptide-induced killing; insertion into bacterial membranes. (A) Barrel-stave model. (B) Carpet model. (C) Toroidal model. Note: hydrophilic regions shown in red, hydrophobic regions shown in blue. Figure adapted from Reference 5.

1.2 Peptide Design: Backbone Mutagenesis

1.2.1 Overview

The chemical mutation of peptides can not only provide us with mechanistic information critical to the field of peptide-based drug design, but may also prove beneficial to the system by increasing the stability of the peptide and enhancing

enzymatic stability. There are several strategies of drug design, however, many factors are to be considered. As previously mentioned, the environments within which they will be analyzed and utilized are both important. One must also think about the protein conformation and folding tendencies before introducing mutations.

The secondary and tertiary structures of proteins are the result of noncovalent interactions within the chain. Though they are quantitatively lower in energy than covalent bonds, these weak intramolecular forces provide substantial stabilizing effects on protein assemblies, in addition to governing their conformation specificity. Examples of noncovalent interactions include ionic interactions, hydrophobic interactions, van der Waals interactions, and of particular interest, hydrogen bonding.[6]

Hydrogen bonding (H-bonding) is a prominent feature within folded proteins, as it dictates to a large degree the protein's folding and stability. Within a native protein, the number of hydrogen bonds is maximized.[6] Disturbing the hydrogen bonding network within a protein can be detrimental to its native form, or conversely can prove advantageous for the system.

A backbone amide bond participates in a H-bonding interaction with the side chains and/or backbone of neighboring residues. Configured with the character of a *trans* double bond, the amide bond orients the H-bond donor (N-H) diametrically opposite from its partner, the H-bond acceptor (C=O). As a result of the π-conjugation of the amide bond, the flexibility of the peptide is limited, thus constricting its rotation and torsion angles, φ and ψ, however H-bonding potential is increased. The secondary structure of a peptide is controlled by these rotational boundaries, as well as steric

restrictions, and is stabilized by hydrogen bonds formed between main-chain peptide groups.[8]

In a study involving ten well-refined proteins, it was observed that only 11% of C=O groups and 12% of N-H groups did not participate in any obvious hydrogen bonding contact. It was also found that main-chain to main-chain carbonyl to amide proton interactions were most predominate: 68% of the donors were N-H and 46% were accepted by C=O. This study proved that main-chain hydrogen bonding interactions weigh most heavily in contribution to secondary structure. Focus on side-chain interactions, then, is lessened and backbone modification studies become more crucial. Through peptide backbone engineering, the hydrogen bonding scaffold can be altered and used to probe the protein's behavior.[8]

1.2.2 Conversion of an Amide to an *E*-Olefin

One option for amide-bond mutagenesis is the conversion to an *E*-olefin (Figure 1.3). This alkene moiety perturbs the H-bonding network by eliminating both a backbone H-bond acceptor and donor. Though the synthesis is challenging, its outcome could contribute substantially to peptide design. The isosteric mutation increases the hydrophobicity of the peptide, which could in turn increase membrane permeability and possibly potency. The outcome of such a transformation is governed by several factors that must be considered. Both entropic and enthalpic contributions play an important role in the peptide's stability.[9]

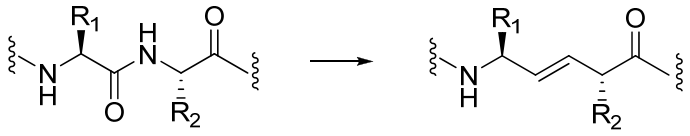

Figure 1.3: Backbone modification of amide bond to *E*-olefin.

Kelly and coworkers have initiated a project to determine the requirements for amyloidogenesis of the amyloid-beta protein by incorportating an *E*-olefin dipeptide isostere into a polypeptide backbone. This enables hydrogen bond perturbation, which could play a significant role in aggregation of the peptides. Using a stereoselective synthesis of the Phe-Phe *E*-olefin isostere, the group successfully prepared a peptide in adequate yield in order to examine the role of hydrogen bonding in protein structure.[9]

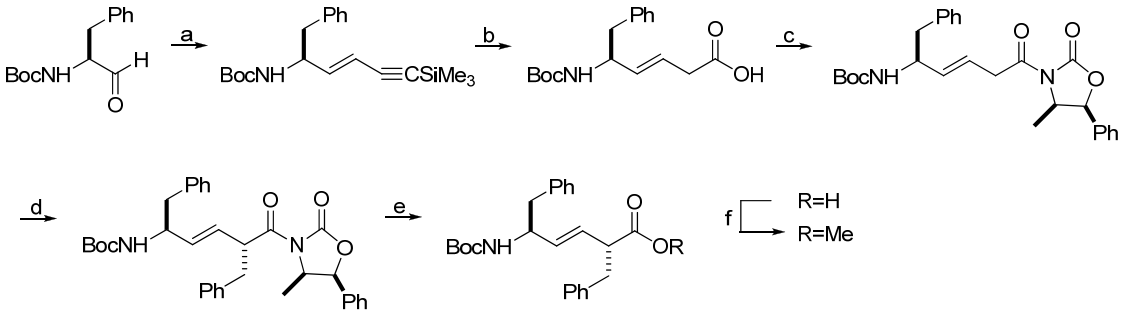

Scheme 1.1: Synthesis of *E*-olefin isostere. Figure adapted from Reference 9.

Scheme 1.1 outlines the chemical synthesis of the desired dipeptide isostere. A Wittig reaction of the amino aldehyde, *N*-Boc-Phe-H, and *n*-BuLi, followed by a hydroboration-oxidation afforded the Phe-Gly isostere. Evan's chiral oxazolidinone was then installed on the C-terminus of the dipeptide, condensing the acid. Finally, the

oxazolidinone enolate was subjected to excess benzyl bromide and diastereolectively alkylated. The structure of the Phe-Phe isostere was confirmed using X-ray crystallography (Figure 1.4).[9]

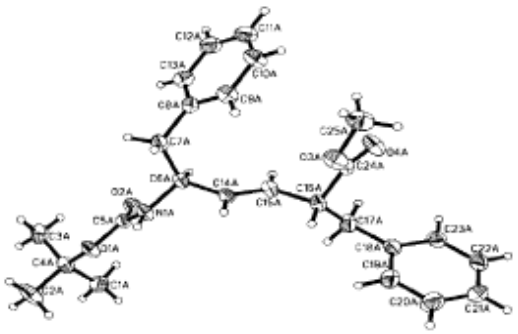

Figure 1.4: The X-ray structure of the Phe-Phe *E*-olefin dipeptide isostere synthesized by the Kelly lab at Scripps. Adapted from Reference 9.

In order to examine the effect of removing both the H-bonding donor (amide proton) and H-bonding acceptor (carbonyl oxygen), the dipeptide was incorporated into the target peptide, Aβ-40 within the central, hydrophobic region (F19,20). Upon this removal, the peptide loses its primary region argued to dictate cross-β-sheet-based amyloid fibrils. Fluorescence experiments employing incubation of the peptide with thioflavin T (an environmentally sensitive fluor that binds and fluoresces when bound to spherical and cross-β-sheet aggregates of Aβ) showed that the mutant peptide was able to self-assemble. Circular dichroism was used to examine secondary structure, though results were somewhat inconclusive. Atomic force microscopy was then used, proving

that no fibril formation was observed within the mutant. They proved that the backbone modification indeed prevented the formation of spherical aggregates into fibrils.[9]

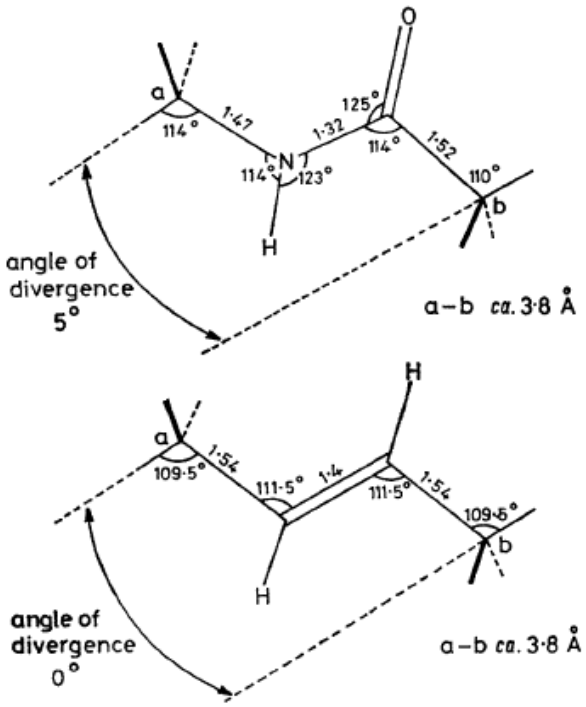

Figure 1.5: Spatial disposition of amide and *trans*-olefin bonds. Distances in Å. Adapted from Reference 10.

Olefin installation in peptides is not a new approach. Research on these double bond isosteres has been carried out for several decades for several other purposes.[10, 11] Sammes and coworkers explored routes to peptide analogues using *trans*-carbon-carbon double bonds for use in Leu-enkephalin analogue synthesis. He proposed this to be a favorable isosteric replacement for it avoided use of D-amino acids so the spatial disposition of the natural peptide was not altered (Figure 1.5). Sammes hoped to use these analogues as peptidase inhibitors due to their high inhibitive efficacy.[10] Later on, his team targeted two additional peptide analogues with new goals: (i) in order to provide stability

and prevent enzymatic hydrolysis of the amide bond within MIF (melanocyte stimulating hormone release inhibiting factor), while retaining biological activity, the amide bond was replaced with the alkene functionality; (ii) in hopes of creating a double bond mimic of the D-Ala-D-Ala dipeptide, a unit used in bacterial cell wall synthesis (Figure 1.6). The preparation of the di- and tri-peptides incorporating proline and alanine analogues used a similar synthetic approach to Kelly consisting of hydroboration-oxidation of conjugated enynes to form βγ-unsaturated acids which are selectively alkylated to furnish the backbone with a second functionality.[11]

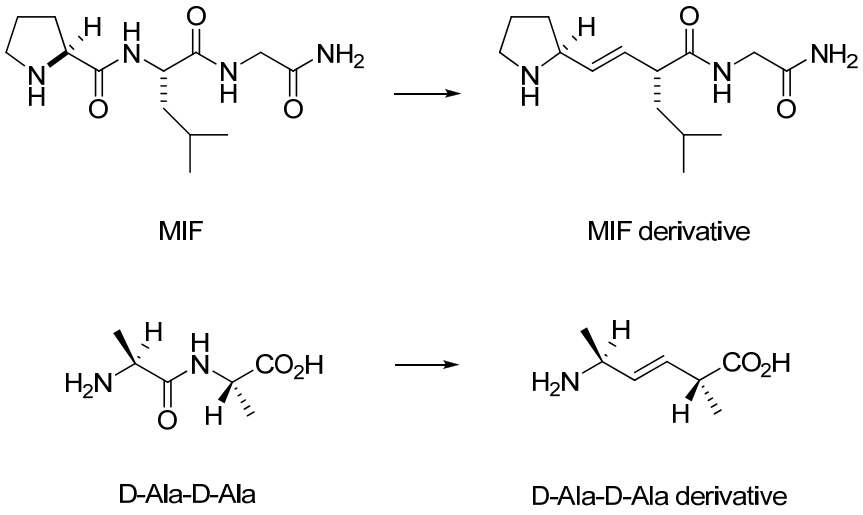

Figure 1.6: Synthetic targets generated using direct alkylation by Sammes, Miles, et al. Figure adapted from Reference 11.

1.2.3 Conversion of an Amide to an Ester

Another option for backbone modification is the replacement of an amide bond with an ester bond. Ester linkages within the peptide backbone were predicted to be an

advantageous modification due to the conservative nature of mutation. Potential downfalls could be the increased flexibility around the ester linkage, as well as the differing electronic properties and solvation. For these reasons, more concrete data about the hydrogen bond strengths were of great interest. Synthesis of FmocProOGly was achieved in a three-step process in low yield, however, sufficient enough to incorporate into the peptide [$(ProProGly)_4ProProOGly(ProProGly)_5$] upon condensation of dipeptide segments.[12]

To examine the effects of the amide to ester bond mutations, a very commonly known triple-helical protein, collagen, was used. Incorporation into the helix showed that the *E*-olefin replacement of the amide bond was in fact unfavorable, especially in comparison to an ester mutation as determined through circular dichroism and thermal melting experiments assessing helical stability and ellipticity. The ester has been shown to induce minimal structural perturbations. Hydrogen bond strengths were estimated to be approximately 2.0 kcal/mol. The alkene moiety, however, did not appear to be a sufficient substitute of the amide bond in this situation, and was a much less stable surrogate. Proposed rationale to this observation includes unfavorable φ and ψ torsion angles for triple helix formation, low dipole moment, decreased solvation, etc. It is clear that the native secondary structure determines the compatibility of the *E*-olefin within the protein. Accommodation of the isostere is generally greater for β-sheets and β-hairpins, as opposed to α-helices.[12]

Though the stability of an ester bond within a peptide is less than that of the native backbone amide, more susceptible to proteolytic and hydrolytic cleavage, the

mutation could help the understanding of the mechanistic properties of peptides that could potentially serve as therapeutic agents.

1.2.4 Conversion of an Amide to a Thioamide

A third alternative is the incorporation of a thioamide into a peptide backbone (Figure 1.7). Conversion of the carbonyl of an amide bond to a thiocarbonyl has several effects on the stability of a peptide. Though it is a nearly isosteric replacement, characteristics of the amide bond are slightly altered. The sulfur atom has an increased steric bulk with respect to oxygen, radii differing approximately 45 pm (65 pm for O, 109 pm for S). Sulfur is also slightly less electronegative than oxygen. Consequently, the hydrogen bonding properties are altered. The thiocarbonyl (sulfur atom) becomes a weaker hydrogen bond acceptor, while the hydrogen bonding properties of the amide proton become stronger. Figure 1.8 displays the steric differences between an amide and thioamide linkage.

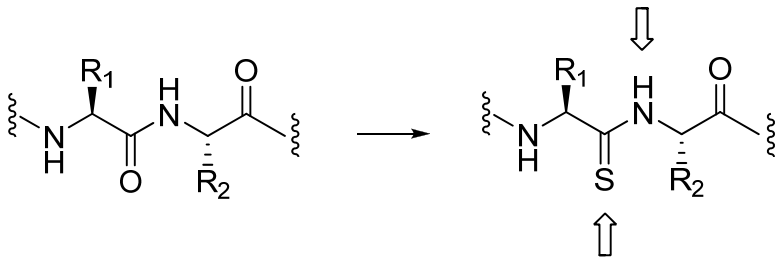

Figure 1.7: Conversion of amide bond to thioamide linkage. Arrows indicate the position of changes in the H-bonding donor (N-H) and acceptor (C=S).

The investigation of the stability of helical peptides containing a thioamide linkage has been carried out by Julia Miwa from Wellesley College. Several predictions were made prior to their study with respect to the effects of the sulfur atom in the hydrogen bonding network. Two possible scenarios proposed were (i) the hydrogen bonding network will be perturbed and α-helix formation will be prevented, or (ii) the helix will fold with a distortion at the thioamide region while excluding the sulfur from the hydrogen bonding network. Positioning at the C-terminal region of the helix should pose no disruption because the last four residues do not participate in H-bonding.[13]

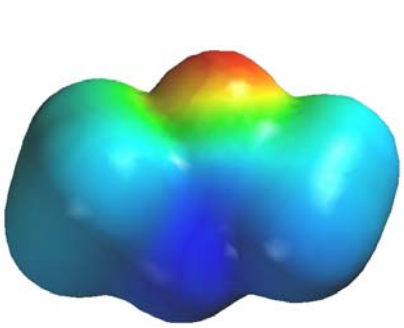

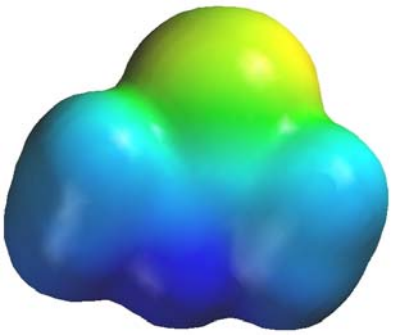

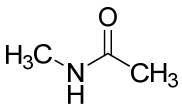

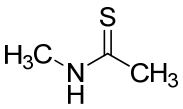

112.63	**Surface Area (Å^2)**	121.69
80.28	**Volume (Å^3)**	88.96
-0.605	**Partial Charge (=O, S)**	-0.496
0.320	**Electrostatic Charge (-NH)**	0.175

Figure 1.8: Spartan images and analysis of the spatial orientation of an amide versus a thioamide bond.

Miwa tested these hypotheses with sedimentation equilibrium and CD experiments that showed that the peptides preferentially fold into parallel α-helical coiled structures nearly identical to their native structure. They were able to show a substantial compatibility of the mutation at different locations within the helix, as well as at the C-terminus (Figure 1.9), proving that the relative stability between mutants and wild-type were comparable.[13]

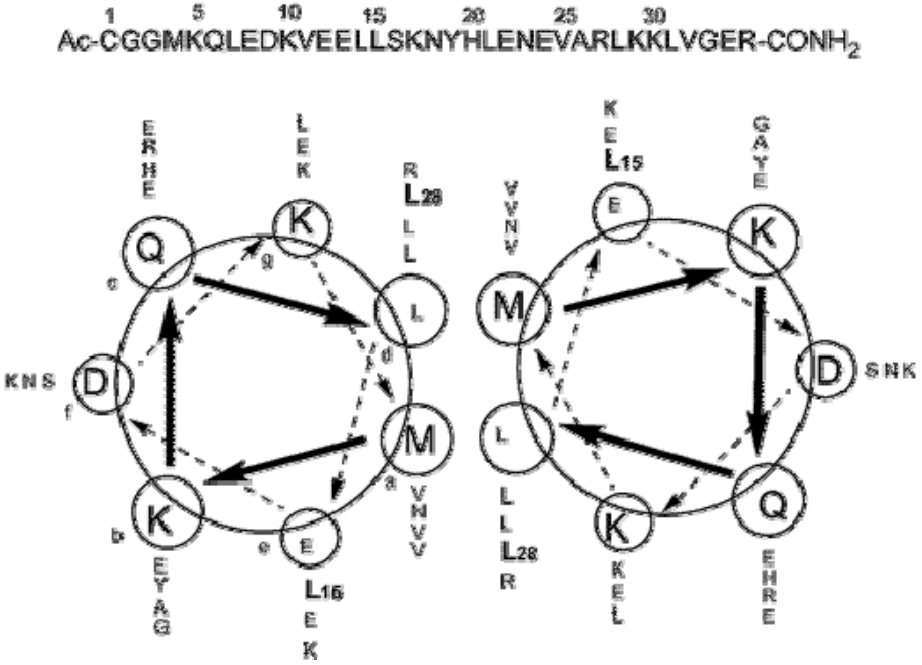

Figure 1.9: Sequence and helical wheel diagram of thioamide linkages incorporated into two different locations: Leu-15 and Leu-28, replacing the carbonyl oxygen with sulfur.[13]

Previous to this work, Miwa studied the effects of thioamide linkages within β-sheet conformations, specifically β-hairpins. The mutation was made within the type II' β-turn region of the hairpin, allowing the *N*-thioacyl amino acid to adopt the extended

conformation required for an antiparallel β-sheet, positioning the sulfur toward the exterior of the hairpin. The amide proton, however, still serves as a H-bond donor. Using two-dimensional NMR (specifically ROESY) to analyze long-range NOEs and COSY and TOCSY for resonance assignments, as well as circular dichroism spectroscopy to analyze the conformation of the peptide, they proved the persistence of a very similar hairpin conformation to that of the oxo peptide, however, no information on the relative stability is reported.[14]

Peptides used by Miwa were synthesized using Fmoc solid-phase synthesis, while performing thioacylation within the peptide using Fmoc-Gly-thioxo-6-nitrobenzotriazolide.[13] Similarly, Rapoport and group from the Lawrence Berkeley National Laboratory at the University of California have developed a method using a nitrobenzotriazole as a thioacylating agent. The three-step reaction sequence shown below in Scheme 1.2 involves the coupling of 4-nitro-1,2-phenylenediamine with a *N*-Boc amino acid, followed by direct thionation using phosphorus pentasulfide in basic conditions. The synthesis is completed with an intramolecular diazonium cyclization using nitrous acid generated *in situ*. To test their thioacylating efficiency, the benzotriazole was coupled with α-methylbenzylamine, which produced the desired coupling product in high yield and enantiomeric purity.[15]

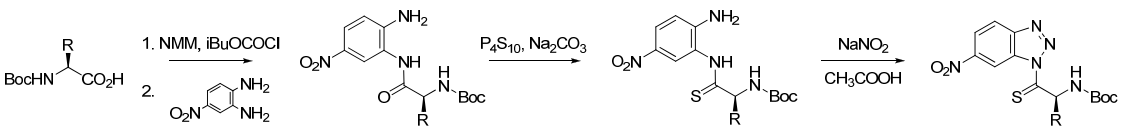

Scheme 1.2: Synthesis of benzotriazoles designed by Rapoport. Figure adapted from Reference 15.

Studies using thioamide bond mutations are advantageous to the field of peptide-based drug design because of their structural similarity to the native backbone amide. Mutants can not only help to probe mechanisms, but can more importantly help enhance the enzymatic stability of peptides.

1.2.5 Additional Heterogeneous Backbones

As research in this field became increasingly intriguing and important, many others joined in pursuit of peptide drug design. Over the last decade, Samuel Gellman has made enormous progress in the field of heterogeneous backbones within a variety of foldamers. Foldamers are non-natural oligomers that display discrete folding propensities, and thus have the potential to exhibit biopolymer-like conformational tendencies, proving a sufficient mimic of various protein systems. Gellman proposed that foldamers were an ideal platform to study structure-activity relationships among peptides and their analogues. Backbones containing both α- and β-amino acids have been a main focus of study (see Figure 1.10). To expand the backbone artillery, several forms of the β-amino acids are used, including protein-like side chains and even cyclic structures for rigidity. Since new antimicrobial agents are in great need, the ability to synthesize peptides to directly mimic naturally occurring host-defense peptides is desirable and could lead to a variety of potential biomedical applications. Furthermore, success in Gellman's project could have a profound impact on modern chemistry and medicine.[16]

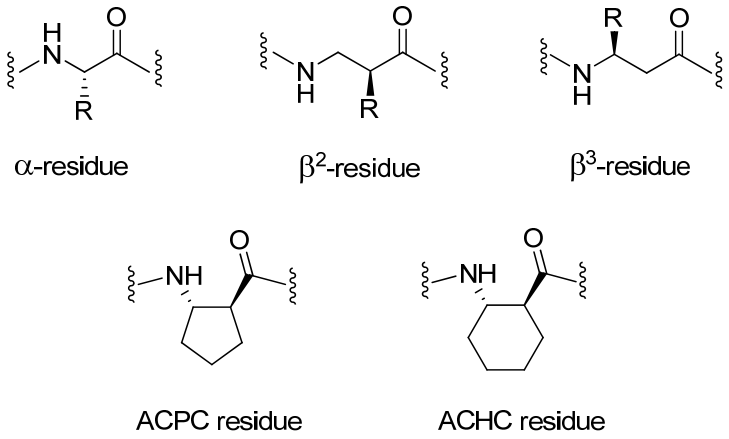

Figure 1.10: Various β-residues used in heterogeneous backbone. Figure adapted from Reference 16.

1.3 Experimental Goals

Chemical mutation will be used to study the structure formation and membrane-lytic mechanism of a variety of peptides in order to expand the scope of peptide-based drug design and improve upon the drug-likeness of antimicrobial peptides. Key research goals include (i) improving the protease resistance of peptide therapeutics in order to alleviate delivery via injection and (ii) improving the potency of peptide therapeutics by tuning the conformation to its functional form and disfavoring the nonfunctional conformation. Thioamide linkages will be installed into a variety of peptides, and several analytical tools will be used to assess the outcome of the mutation on the structure and function of the peptides.

1.3.1 Structural Effects of Thioamides in Soluble Peptides

By incorporating thioamide linkages into a variety of soluble peptides, we hope to quantify their effects in protein conformation and stabilization. Examples of the systems that will be studied include the well known peptides gb1 and Trpzip 4. Circular dichroism and ^{1}H-NMR are two main tools that will be used to measure the stabilities of the mutant peptides.

1.3.2 Thioamides in Gramicidin A: Effects on Channel Formation

Gramicidin A is a well-studied peptide with significant bactericidal activity as a result of its permeability into bacterial cell membranes. This peptide is thus optimal for studying the structure and function of membrane proteins. Gramicidin A is a 15-residue hydrophobic peptide composed of alternating sequence of D- and L-amino acids that exists in two major conformations: a β-helical ion channel and an intertwined double-helical structure, the non-channel form.[17] The interconversion of the two conformations is an interesting area of study. Thioamide linkages will be introduced into Gramicidin A in order to test the conformational preference of the peptide. The effects of the mutation in antimicrobial peptide design will be analyzed.

CHAPTER 2

Results and Discussion

2.1 Synthesis of Thiolating Amino Acids

Thiopeptides were prepared using organic synthetic schemes similar to that employed by Rapoport in his studies of thioacylating reagents.[15] First, the mixed carbonic anhydride methodology for peptide synthesis was employed in order to couple the *N*-Fmoc amino acid with 4-nitro-1,2-phenylenediamine. Next, the conversion of the carbonyl to a thiocarbonyl was accomplished by direct thionation using phosphorus pentasulfide and sodium carbonate. After purification of the thioamide, an intramolecular diazonium cyclization using nitrous acid generated *in situ* with sodium nitrite and acetic acid yielded the final product. Amino acid derivatives synthesized were tryptophan, phenylalanine, glycine, and D-leucine in varying yields (42-69%). This method, shown in Scheme 2.1, proved versatile for a range of amino acids, as well as being a short and efficient route. The

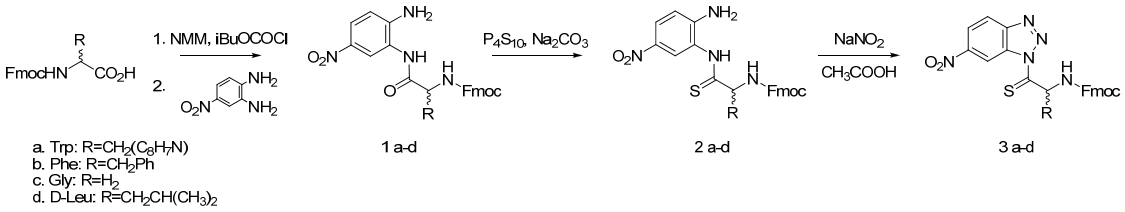

Scheme 2.1: Synthesis of Benzotriazole Thioacylating Agents used Directly in SPPS.

incorporation of the thioamide into the molecule was verified after thionation based on a characteristic resonance between 200-213 ppm in the ^{13}C-NMR spectrum (Figure 2.1). The puritiy of each amino acid derivative was also confirmed using HR-MS.

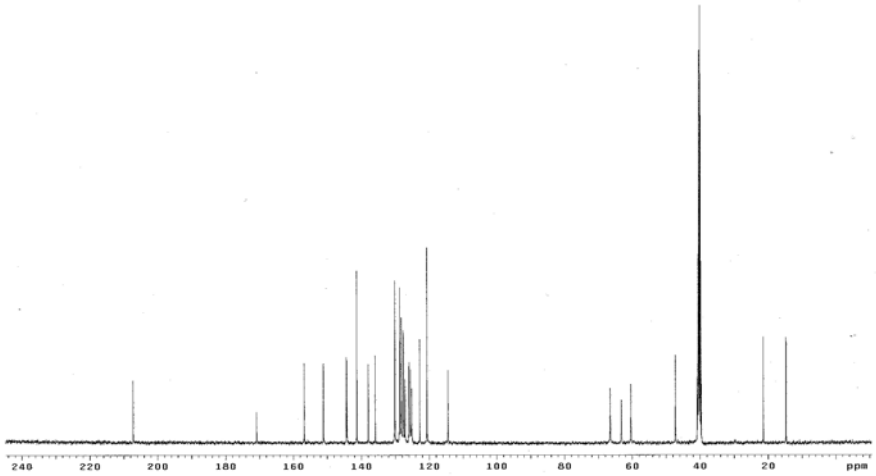

Figure 2.1: Sample ^{13}C-NMR spectra of **2b** proving the incorporation of the sulfur carbonyl based on the characteristic resonance at 207.3 ppm.

2.2 Thioamides in Soluble β-Hairpins

In order to investigate the effects of a thioamide linkage within a protein, an ideal model system had to be chosen. The simplest structural protein motif is the β-hairpin, comprised of two beta strands adjacent in primary structure oriented in an antiparallel arrangement linked by a short loop of two to five amino acid residues. These hairpins can exist on their own or can contribute to a larger protein structure such as a beta sheet or globular proteins. Given that hairpins are typically short, ranging from 10-20 amino acids, the complexity of analyzing the system is minimized in comparison to larger proteins. It was thus crucial to find a suitable β-hairpin to introduce thioamide linkages at various positions in order to understand their contributions to the overall peptide structure.

One system of study was gb1, a β-hairpin peptide taken from the B1 IgG-binding domain of protein G. Gb1 has been shown to exhibit partial hairpin character, approximately 40% determined by NMR.[18]

PEPTIDE	SEQUENCE	DETAILS
gb1, 41-56	GEWTYDDATKTFTVTE	Type I turn
Trpzip 4	GEWTWDDATKTWTWTE	gb1: Y45W, F52W, V54W

Table 2.1: Sequences of Trpzip 4 and gb1, allowing for comparable peptide systems.

It is hypothesized that the installation of a thioamide linkage would enhance the stability within the peptide, making gb1 a suitable system to detect the effects of the mutation. In order to validate this hypothesis, both wild-type gb1 and thioamide mutant F12*Fgb1 were synthesized using solid-phase peptide synthesis (SPPS). The Phe-benzotriazole was directly incorporated into SPPS. After peptides were synthesized and purified via RP-HPLC, concentrations were calibrated using UV/Vis spectroscopy, and samples were tested using CD to assess the secondary structures of the peptides, as well as their stabilities. Wavelength scans for the peptides were inconclusive, and thermal denaturation was unsuccessful on account of the peptides' low stability. No conclusion could be made about the stability of the thioamide within the gb1(41-56) hairpin.

We then attempted to circumvent this problem with a more stable version of gb1: Trpzip 4. The sequence of Trpzip 4 is a gb1 variant with three mutations (Table 2.1). Tryptophan zippers are a structural motif that provide an unusual amount of stability to the β-hairpin conformation within short peptides due to the cross-strand pairs of indole-rings.[19] Trpzip 4 is an example of such a peptide. Incorporation of a thioamide into the

peptide backbone was accomplished by introduction of a thioacylating reagent (Trp-benzotriazole) as the fifth residue (W5*W-Trpzip 4) during solid phase peptide synthesis. After purification, the structure and stability of the mutant peptide was analyzed.

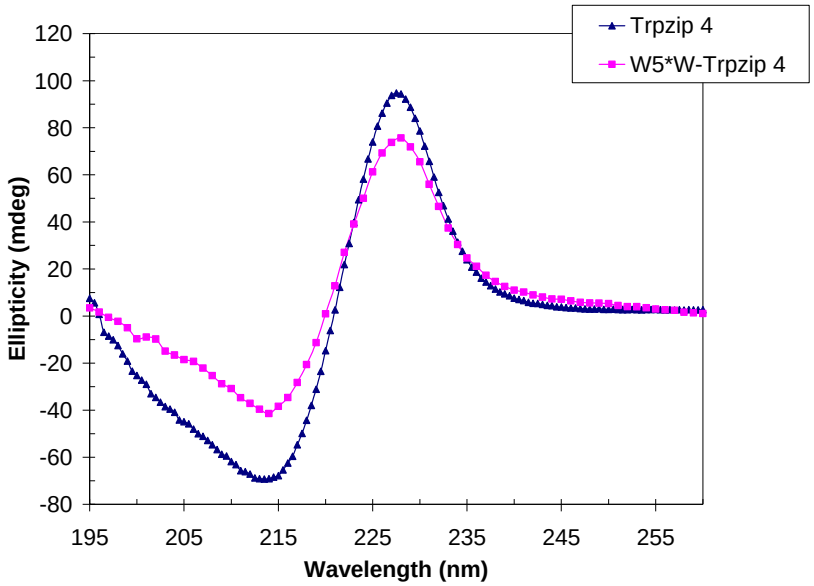

Figure 2.2: CD spectra of wild-type Trpzip 4 versus W5*W-Trpzip 4 (50 μM, 25°C).

First, the secondary structure of the peptide was obtained using circular dichroism (Figure 2.2). Both a maximum at approximately 228 nm (Trp-aromatic interactions) and a minimum at approximately 215 (indicating its beta-character) were observed. The thioamide mutant, W5*W-Trpzip 4, adopted an identical conformation to that of the wild-type peptide.[19]

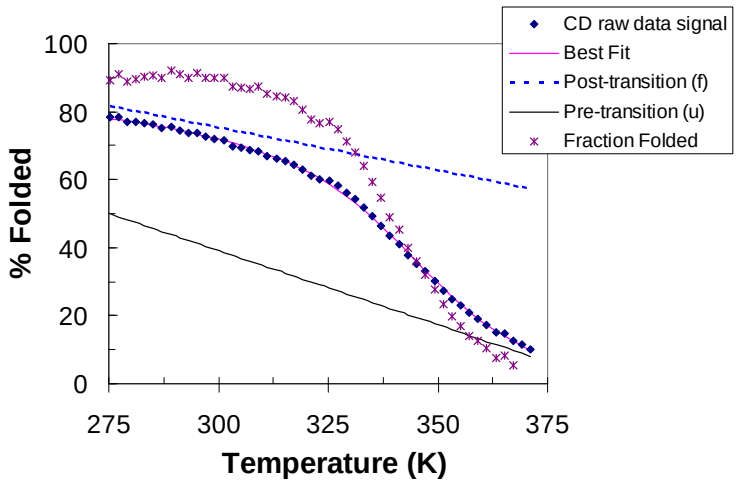

Figure 2.3: Thermal denaturation of W5*W-Trpzip 4 monitored by CD. Melting data was acquired with 50 μM peptide samples in 20 mM sodium phosphate buffer, pH 7.0.

Next, thermodynamic properties of W5*W-Trpzip 4 were analyzed using thermal denaturation data collected by CD spectroscopy (Figure 2.3). Melting temperatures and various thermodynamic parameters were extracted from the data (Table 2.2) and compared to data collected by Cochran for wild-type Trpzip 4.[19] Experimental conditions varied slightly (20 μM samples in potassium phosphate buffers, pH 7.0), however, data remains comparable.

	Trpzip 4	**W5*W-Trpzip 4**
T_m, K	343	339
ΔH_m, kcal·mol^{-1}	21.9	19.7
ΔS_m, cal·mol^{-1}·K^{-1}	63.7	58.2
ΔC_p, cal·mol^{-1}·K^{-1}	380	409
ΔG_f, kcal·mol^{-1}	-1.25	-1.33

Table 2.2: Thermal unfolding analysis of Trpzip 4 and W5*W-Trpzip 4.

It is evident that data obtained from the thermal melts show the mutant and wild-type peptides to be very similar in their melting temperatures, entropic and enthalpic values, and the heat capacity. Furthermore, both structural and thermodynamic data prove that the thioamide linkage was well-accommodated within the tryptophan zipper and the peptide exhibited comparable stability to the native conformation of the wild-type.

Another peptide system and a new set of analytical tools were used for the next study. One appealing technique to quantify peptide folding has been used by Marcey L. Waters in her studies of various aromatic interactions within β-hairpins.[20, 21] Since the extent of folding in a β-hairpin directly correlates to the separation of the glycine H_α resonances, ^{1}H-NMR spectroscopy can be used for analysis. A simple calculation can then determine the population of folded peptide. Shown below is the equation used by Water's, where the fraction folded is equal to the difference in the chemical shift of the

observed peptide versus the random coil control divided by the difference in the chemical shift of the fully folded and random coil control.[20] This formula is followed by the simplified equation, mathematically derived from Water's data by Kristofer Comeforo, directly used in this study, where x = $\Delta\delta$ Gly-H_α. Thus, the fraction of peptide folded can be found directly using ^{1}H-NMR spectra.

$$F_f = \left[\frac{\delta_{obs} - \delta_0}{\delta_{100} - \delta_0}\right] \quad \Rightarrow \quad \left[\frac{x + 0.01000598}{0.575}\right]$$

Equation 2.1: Fraction of peptide folded

In order to utilize this strategy employed by Waters, peptide design is quite imperative. The peptide sequence used by Waters (Figure 2.4),[20-22] modified from a β-hairpin originally developed by Gellman and co-workers,[23] was adopted as it appeared to be an adequate system for this study (Ac-RFVOVNGKEIFQ-NH_2). Several factors must be considered when deciding upon a peptide system, such as solubility, preferred conformation, etc. The chosen peptide has a net charge of +2 which is not only optimal for solubility enhancement, but also for aggregation prevention. Also, the turn region contains an Asn-Gly moiety known to readily induce a type I' turn for β-hairpin formation.[20]

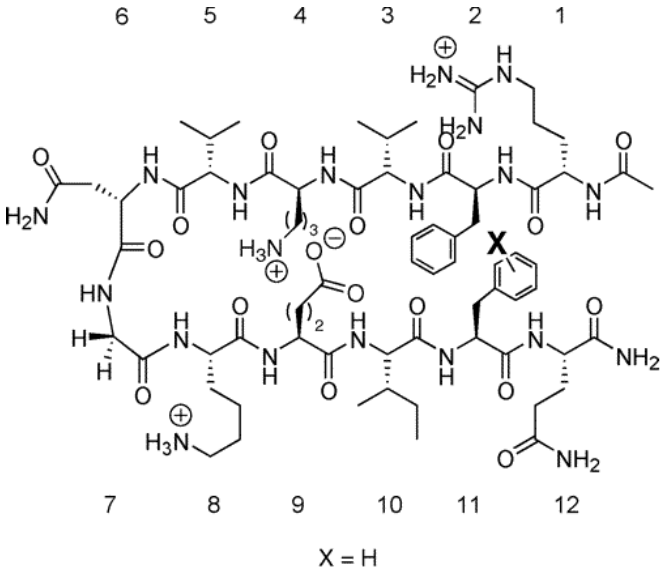

Figure 2.4: Peptide sequence used to probe the influence of the incorporation of a thioamide linkage within the backbone of a β-hairpin.[21]

Phenylalanine seemed to be an appropriate target for the incorporation of the thioamide linkage because of its relative location within the peptide. Because the behavior of the glycine residue is the probe for the study, the turn region was avoided, and thus the Phe residue (position 2) within the C-terminal beta strand was chosen. The peptides were synthesized using Fmoc-strategies with solid phase peptide synthesis (SPPS) and purified using reverse-phase HPLC. Masses were confirmed using LC-MS.

β-Hairpin Sequence	% Folded	ΔG_f (kcal·mol$^{-1)}$
Ac-RFVOVNGKEIFQ-NH_2	39	0.25
Ac-R*FVOVNGKEIFQ-NH_2	55	-0.11

Table 2.3: β-hairpin Stabilities Determined from Glycine Chemical Shifts at 295 K.

The peptides were then subjected to ^{1}H-NMR experiments in D_2O/AcOD buffer (pH 5.0) to compare the structural integrity of the wild-type peptide versus its thioamide mutant F2*F-MW-β-hairpin. The experimental data collected at 22°C is shown in Table 2.3. Note that since these peptides interconvert between folded and unfolded conformations rapidly on the NMR time scale, the data collected in the form of chemical shifts is actually the average of the folded and unfolded states.

Because of the simple mutation of an oxygen to a sulfur carbonyl, the native behavior of the peptide was altered. Sulfur has a larger atomic radius than oxygen, thus one could predict that its increased steric bulk could introduce a folding barrier within a β-hairpin. Accommodating the increased size could compromise its foldedness, however, in this β-hairpin, it was in fact enhanced. Data obtained at 22°C clearly indicates that the thioamide linkage provided additional stability to the peptide, increasing β-sheet propensity. The benefit of the strengthened H-bond donor on account of the electron-withdrawing strength of the carbonyl sulfur was clearly displayed.

2.3 Thioamides in Antimicrobial Peptides: Gramicidin A

Since it was proven that a thioamide within Waters' β-hairpin boosted the peptide's stability, it would be beneficial to investigate its role within another system. Gramicidin A (gA), a well-studied peptide, is an optimal system for studying the structure and function of membrane proteins. Gramicidin A is a 15-residue hydrophobic peptide composed of alternating sequence of D- and L-amino acids: Formyl-L-Val[1]-Gly[2]-L-Ala[3]-D-Leu[4]-L-Ala[5]-D-Val[6]-L-Val[7]-D-Val[8]-L-Trp[9]-D-Leu[10]-L-Trp[11]-D-Leu[12]-L-Trp[13]-D-Leu[14]-L-Trp[15]-ethanolamine. There are two well-known native conformations of gA (Figure 2.5). The first conformation is where two right-handed beta-helical monomers orient themselves N-terminus to N-terminus forming a monovalent cation selective channel in lipid bilayers (right).[17] The second conformation is an intertwined double-helical structure, also called the double-stranded dimer (left). It is believed to be a misfolded form of gA with no apparent channel activity. The interconversion of the two conformations is an interesting area of study, and furthermore, gA serves as a perfect system to analyze the factors most influential on its conformation as probed by SEC-HPLC, CD, UV/Vis, fluorescence, TLC, etc.[17, 24-28]

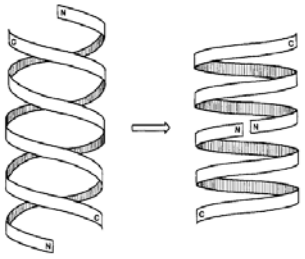

Figure 2.5: A schematic drawing of the gramicidin backbone illustrating some of the salient features for the conversion of double-stranded dimer to a beta-helical channel.[17]

Conformation of gA has been proven to be highly solvent-dependent, but other features of the peptide can be easily probed in order to investigate its behavior in greater detail. This provides a perfect foundation for the incorporation of the thiopeptides. By perturbing the hydrogen-bonding network, the conformation of the peptide could be altered, either favorable or unfavorably.

Again, it was essential to select a position within the peptide where the amide proton is a participant in the hydrogen bonding network, but the thioamide is not, therefore, the steric bulk of the sulfur atom does not provide an additional factor to perturb the system. Because the amide proton becomes a stronger hydrogen bond donor, the intermolecular forces within the peptide are changed which may or may not be accompanied by a conformation change.

Gramicidin A contains four tryptophan residues (9, 11, 13, 15). Tryptophan is an abundant amino acid within membrane proteins, including many other ion channels. This amino acid tends to cluster near the membrane-water interfacial region of transmembrane domains of the proteins. Its hydrogen bonding ability, permanent dipole moment, and large aromatic ring play an important role in both its structure and function, mainly due to its high accessibility for π-π and cation-π interactions.[29] It was part of this experimental design to synthesize both wild-type (WTgA) and a di-phenlyalanine mutant (W9,11FgA), which functions as a control to validate the experimental methods. It is known that the wild-type exists predominantly in the monomeric form, whereas the double mutant exists in some ratio of the two forms, channel and non-channel.

Then, the thiopeptides were introduced into gA containing the double phenylalanine mutation. Positions 10 and 12, both D-Leucine residues, were targeted,

providing two thioamide (T) mutants: W9,11FgAT10 and W9,11FgAT12. Again, at each of these positions within the channel conformation, the carbonyl is oriented outward to accommodate the sulfur atom's steric bulk, and the amide proton is donated within the H-bonding network. This, however, is disfavored in the non-channel conformation because both the carbonyl and amide proton are engaged in hydrogen bonds within the double-stranded dimer (Figure 2.6). The size of the sulfur atom, therefore, would perturb the H-bonding network.

Gramicidin A and mutants were synthesized guided by published procedures[27] using Fmoc chemistry by SPPS on a preloaded Trp-Wang resin. *N*-Formyl-valine was synthesized and purified via organic synthesis and recrystallization. The thiopeptide was introduced into the peptide at the selected position in DMF. Coupling time for benzotriazoles was extended and monitored using UV/Vis spectroscopy.[30] Once the coupling of benzotriazoles exceeded 90%, the peptides were capped by acetylation (10% acetic anhydride in DMF, 1 hour at room temperature), after which peptide synthesis was allowed to complete (natural amino acid coupling >99%). The peptide was cleaved from the resin using distilled ethanolamine, providing the functionalized C-terminus. Precipitation in methanol with water, followed by centrifugation, and finally lyophilization, afforded the peptide as a white powder. Purity and chemical integrity were confirmed with LC-MS.

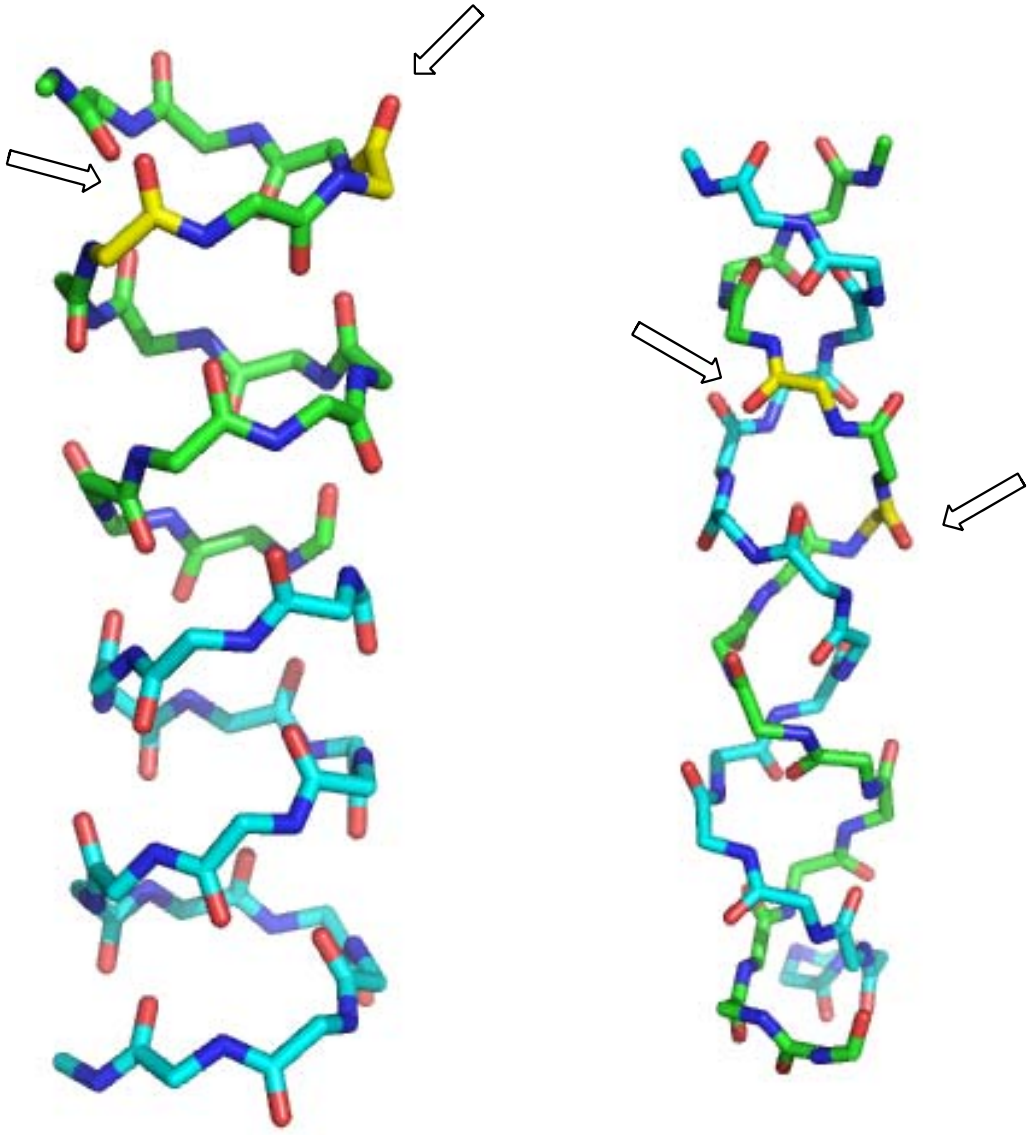

Figure 2.6: Mutated residues of gA dimers (D-Leu^{10,12}) shown in yellow. Channel conformation of gA (left) with the second monomeric subunit shown in cyan with side chains. Note: carbonyl is oriented away from the channel. Non-channel conformation (right) with the second gA strand shown in cyan. Note, carbonyl engages in hydrogen bonding.

To understand the behavior of the peptides, several methods were used, including size exclusion high performance liquid chromatography (SEC-HPLC) and circular dichroism. As previously mentioned, the molecular structure and dynamics of gA are strongly environment-sensitive, so all tests were carried out in both polar (methanol) and nonpolar (tetrahydrofuran) solvents.

It would be beneficial to examine the conformation of the peptides in a membrane, but preliminary tests were necessary to confirm their behavior in solution. Previous reports of SEC-HPLC have been used with an isocratic THF eluent to determine the conformation of gA in various solvents.[26-29] Each of the four peptides of interest were dissolved in two different solvents (40 μM) and immediately injected (5 μL) onto the size-exclusion column at room temperature. Elution times and peak integrations (Table 2.4) were monitored as a clear reflection of the preferred conformation under each condition. All experiments were repeated for accuracy.

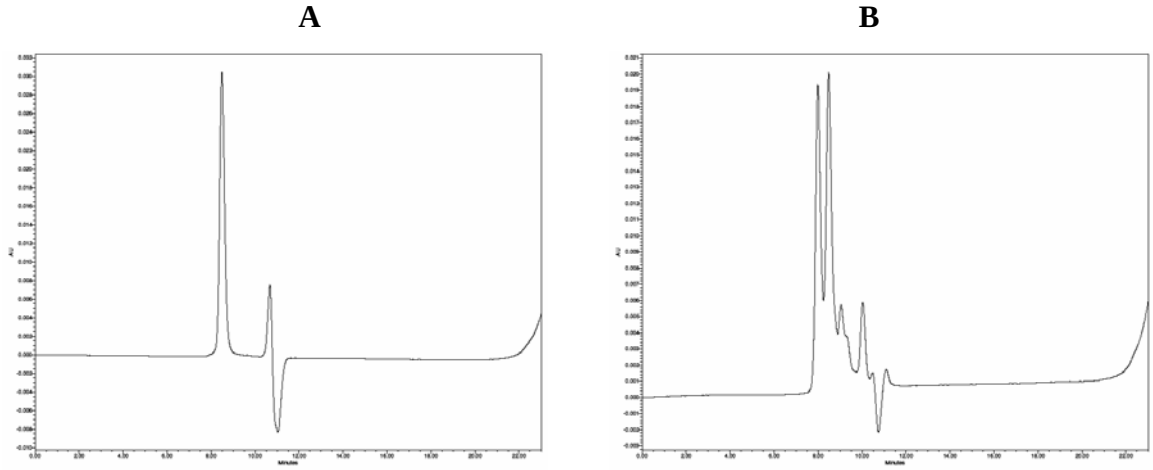

Figure 2.7: Sample traces from SEC-HPLC. (A) WTgA in MeOH; monomer elution at 8.5 min, followed by solvent peaks. (B) WTgA in THF; monomer elution at 8.5 min (52%), dimer elution at 8.0 min (48%).

Sample traces of SEC-HPLC data are shown in Figure 2.7. Data indicates the thioamide mutants gAT10 and gAT12 clearly favor a monomeric structure based on the high percentage of the later elution product (approximately 8.5 minutes) regardless of solvent conditions, whereas WTgA and W9,11FgA show significant percentages of dimer product in THF. It is unknown, however, as to what the actual structure of these monomers and dimers are. Further tests must be carried out to fully characterize the secondary structure of these peptides, specifically when inserted into a membrane.

PEPTIDE	SOLVENT	MONOMER		DIMER	
		Elution Time	%	Elution Time	%
WTgA	THF	8.50	52	8.00	48
	MeOH	8.50	100	--	--
W9,11FgA	THF	8.55	29	8.11	71
	MeOH	8.55	100	--	--
W9,11FgAT10	THF	8.89	94	8.05	6
	MeOH	8.89	100	--	--
W9,11FgAT12	THF	8.50	91	8.05	9
	MeOH	8.50	100	--	--

Table 2.4: SEC-HPLC data collected from 5 μL injections of 40 μM sample eluted with isocratic THF. Monomer/dimer ratios estimated with peak integration.

Circular dichroism was also used as a guide to determine the secondary structure of the peptides. Experiments were run at room temperature in methanol, tetrahydrofuran, and trifluoroethanol (40 μM). Scans were taken after initial dissolvation and 1 hour later to see if there was any conformational change over a short period of time. Traces, however, were somewhat inconclusive due to variances in experimental data in comparison to literature data for the WTgA. Another method was thus attempted to understand the structure of gA and its mutants. ^{1}H-NMR data was collected using samples of the peptides in different solvents (CD_3OH and CD_3OD) in hopes to monitor the Trp amide proton to learn more about its involvement in the H-bonding network, however, exchange was too fast to make any conclusions.

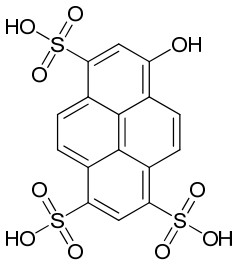

Figure 2.8: Chemical structure of 8-hydroxypyrene-1,3,6-trifulfonate (HPTS).

The final attempt to understand the behavior of these peptides was a functional assay, performing leakage experiments using fluorescence. Liposomes (500 μM) were prepared from DOPC, hydrated with sodium phosphate buffer containing HPTS (8-hydroxypyrene-1,3,6-trisulfonate; Figure 2.8), a hydrophilic pH sensitive dye, and purified using gel filtration (removing external HPTS). They were then exposed to an external environment containing aqueous cesium chloride (10 μM). Sodium hydroxide

(2.5 nM) was titrated into the extravesicular solution, creating a pH gradient of approximately 0.5 pH units across the membrane (pH 7.0 inside, pH 7.5 outside). Once a plateau in fluorescence intensity was achieved, peptide (1.25 μM) was added. Upon titration of the peptide to the solution, internal protons were released from the liposomes, compensated by Cs^+. The internal pH of the liposomes increased because of proton efflux, thus causing deprotonation of the HPTS. See Figures 2.9-2.10.

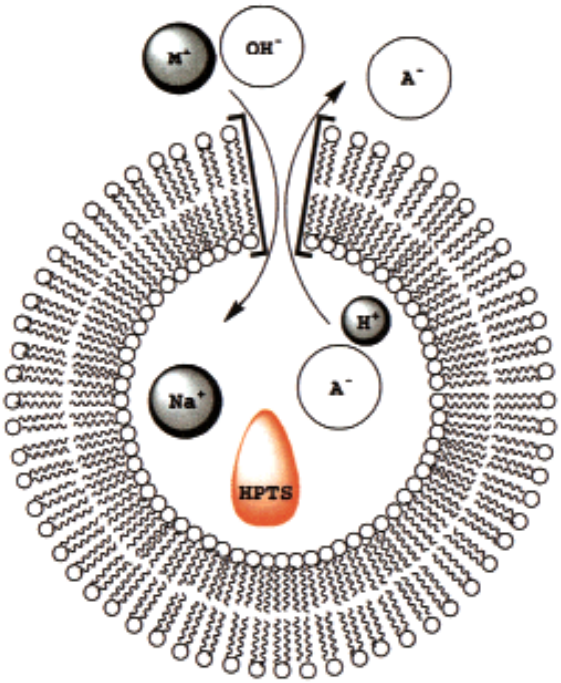

Figure 2.9: Schematic representation of transport experiments. A pH gradient results from addition of extravesicular NaOH solution. The charge caused by H^+ efflux is compensated by cation influx, as mediated by the exogenous ligand, gramicidin A. The increase in intravesicular pH, monitored by the entrapped pH-sensitive dye, HPTS, reflects the electrolyte exchange rate.[31]

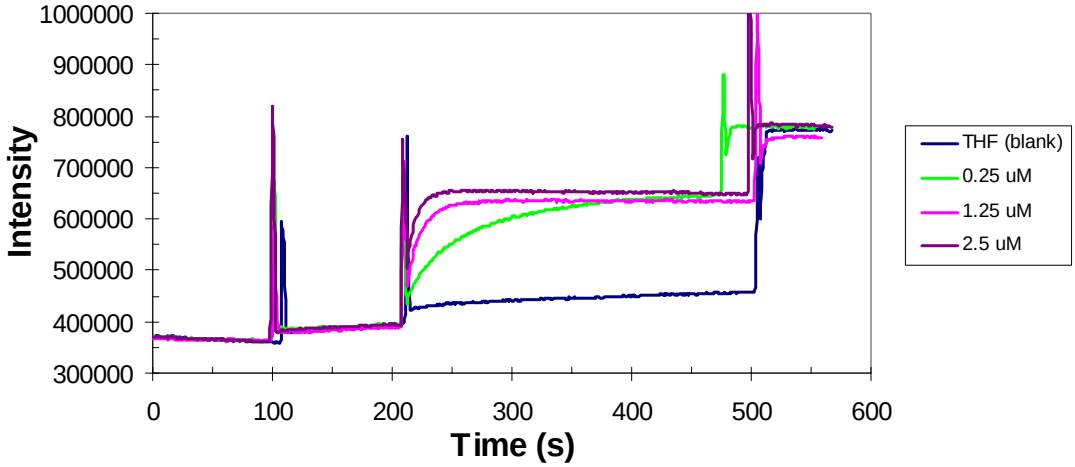

Figure 2.10: Sample fluorescence trace. Note, NaOH addition at 100 seconds, peptide addition shortly after 200 seconds, and finally Triton X-100 addition around 500 seconds.

Transport properties of gramicidin A and mutants were quantified using this technique. Several experiments were performed in order to optimize the conditions for the experiment, as well as collect sufficient data in order to most accurately quantify the results. Fluorescence traces were analyzed quantitatively by probing the kinetics of each peptide. Exponential fits using Origin8 were performed on each curve to determine half-life values. See Figure 2.11.

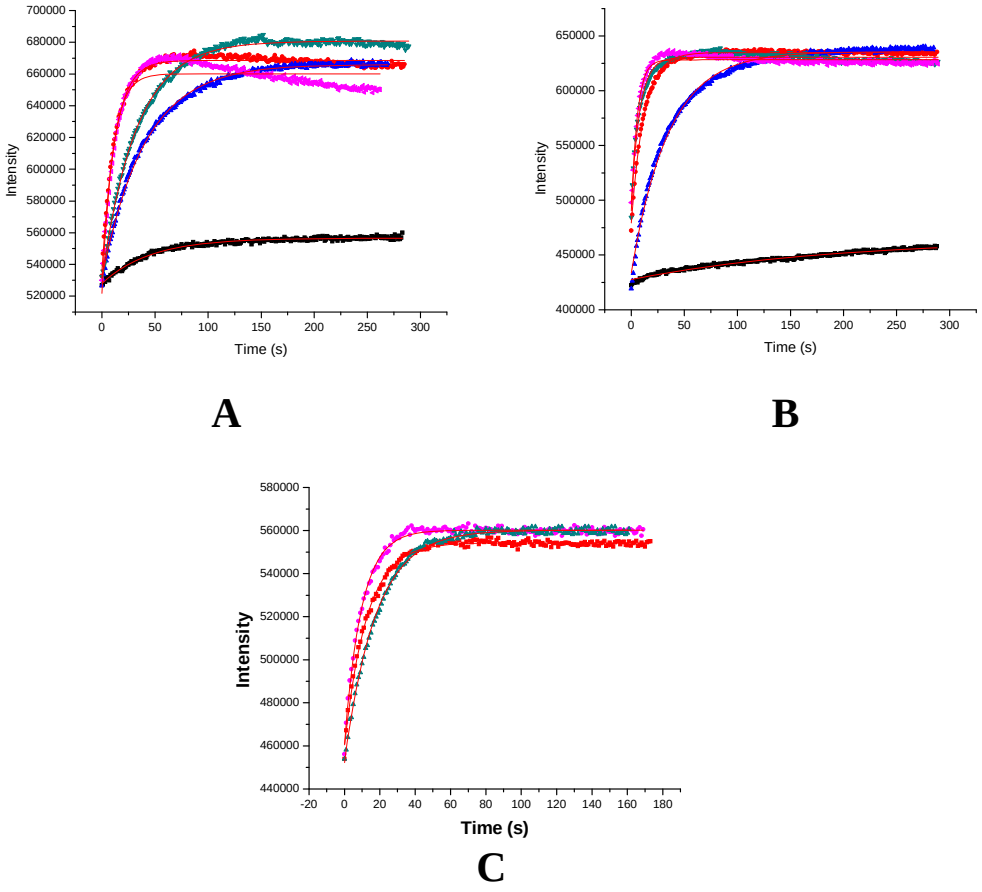

Figure 2.11 A-C: Trials 1-3 of leakage assay monitored by fluorescence. Black trace- THF (blank); Red trace- WTgA; Blue trace- W9,11FgA; Teal trace- W9,11FgAT10; Pink trace- W9,11FgAT12.

	TRIAL 1		TRIAL 2		TRIAL 3		AVERAGE	
PEPTIDE	**$t_{1/2}$**	**Error**	**$t_{1/2}$**	**Error**	**$t_{1/2}$**	**Error**	**$t_{1/2}$**	**Error**
WTgA	12.4	0.17	12.1	0.096	12.7	0.15	12.4	0.14
W9,11FgA	40.6	0.26	35.1	0.31	--	--	37.7	0.29
W9,11FgAT10	33.0	0.23	8.17	0.20	17.6	0.15	19.6	0.19
W9,11FgAT12	10.0	0.43	5.82	0.15	9.68	0.13	8.50	0.24

Table 2.5: Kinetic data from leakage assays monitored by fluorescence.

From the data shown in Table 2.5, we can see that W9,11FgA insertion into the membrane is much slower than WTgA. The thioamide mutants, however, show enhanced channel formation, as indicated by half-lives less than that of the W9,11FgA. W9,11FgAT12, the thioamide mutation at the twelfth position, seems to embed into the liposome at a faster rate than W9,11FgAT10, producing half-lives less than the W9,11FgA and even WTgA. Data clearly show the favorable incorporation of the thioamide linkage into gramicidin A based on its efficiency to cause leakage across a membrane.

Kinetic experiments were run with a final peptide concentration of 1.25 μM, however, to ensure that lipsomes weren't saturated with peptide, detergent was added. Upon Triton X-100 addition, an increase in fluorescence intensity was detected, which was initially interpreted as the point of complete lysis. After analyzing the data from wild-type and mutants, it was suspected that the liposomes may in fact be saturated. Each

peptide resulted in the same maximum intensity (Figure 2.12). Concentration dependence experiments were then carried out, and it became evident that peptides were indeed saturating the liposomes.

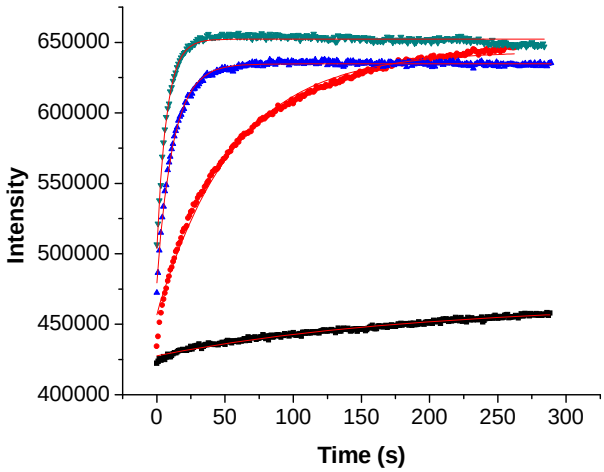

Figure 2.12: Saturation of liposomes with various concentrations of wild-type gramicidin A. Red trace- 250 nM; Blue trace- 25 nM; Teal trace- 2.5 nM; Black trace- THF [blank].

	$t_{1/2}$ (s)	Stnd Error
THF (blank)	190.	8.6
0.25 μM	56.6	0.64
1.25 μM	12.2	0.096
2.5 μM	7.32	0.11

Table 2.6: Half lives of WTgA of varying concentrations calculated from leakage experiments as monitored by fluorescence.

Later experiments with lower concentrations were performed, showing that a more optimal peptide concentration would be on the nanomolar scale (Figure 2.13), where maximal leakage is not achieved until Triton X-100 is added.

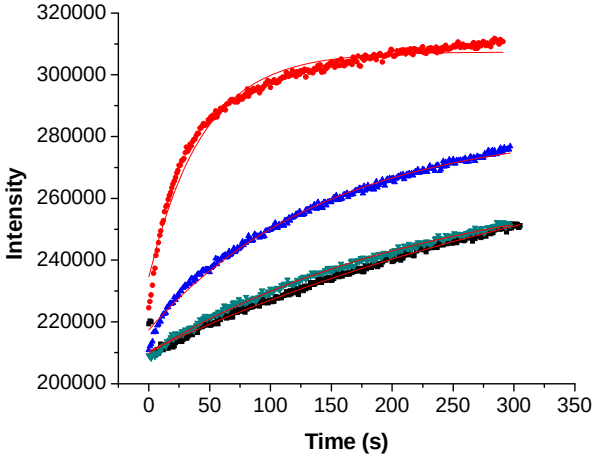

Figure 2.13: Concentration dependence of leakage using wild-type gramicidin A. Red trace- 250 nM; Blue trace- 25 nM; Teal trace- 2.5 nM; Black trace- THF [blank].

	$t_{1/2}$ (s)	Stnd Error
THF (blank)	462	30.
250 nM	44.2	0.82
25 nM	145	2.6
2.5 nM	234	5.4

Table 2.7: Kinetic analysis of concentration dependence of leakage using WTgA. Half-life values reported as calculated from Exponential Fit using Origin8.

Why, then, did the fluorescence intensity increase after addition of detergent? In order to investigate this pattern, phosphate buffer was prepared to best mimic the environment in the previous gA experiments directly before Triton X-100 titration (30 nM HPTS, pH 7.5) and placed in the fluorescence cuvette. The fluorescence intensity was monitored for 100 seconds upon which Triton X-100 was added. Based on the relative change in intensity, it was verified that there is some arbitrary non-specific effect of the detergent on the liposomes, proving saturation was indeed reached with 1.25 μM gA. A mathematical estimation validates this conclusion. If we assume that each liposome contains roughly 50,000 lipid molecules, then the final liposome concentration used in these experiments was approximately 10 nM. Technically only one gA channel is necessary for leakage, and thus at micromolar concentrations of gA, peptide levels are well beyond saturation.

Future experiments may be necessary to better analyze the efficiency of these channel-forming peptides. Not only could a more accurate analysis of kinetics be achieved, but also, it is possible that the thermodynamic analysis would be made accessible by interpreting maximum intensity values. Leakage assays using gA of less than 25 nM would be ideal. Also, the concentration dependence of leakage using each mutant would also be valuable data to obtain.

Once these experiments are completed, it would be interesting to evaluate the proteolytic resistance of these mutant peptides, as well as their antibiotic efficiency in bacterial cells. If we could prove that the thioamide version of gramicidin A improves the enzymatic stability of the peptide, the applications of the mutation will expand dramatically.

CHAPTER 3

Conclusion

Thioamide linkages were installed in a variety of soluble peptides, replacing the backbone amide linkage, in order to quantify the effects on the peptides' conformation and stability. Through thermal melting experiments, the thioamide mutant W5*W-Trpzip 4 showed comparable stability to its wild-type, Trpzip 4, a well-known tryptophan zipper. Using ^{1}H-NMR, it was shown that the thioamide mutant F2*F-MW-β-hairpin was more stable than its wild-type based on the population of folded peptide and the free energy of folding.

Secondly, the efficiency of the channel-forming antimicrobial peptide, gramicidin A, was improved by the respective backbone mutations, W9,11FgAT10 and W9,11FgAT12, as demonstrated by SEC-HPLC and fluorescence experiments. This could be a potential synthetic route to consider when developing AMP-like drug design.

In conclusion, the thioamide mutation was shown to be well-accommodated within peptides with different secondary structures, and thus proved to be a useful and versatile modification. Future studies including similar backbone engineering could be a promising field and will hopefully make significant contributions to the field of peptide drug design.

CHAPTER 4

Experimental

General Methods: Synthesis of Thioacylating Reagents

All ^{1}H-NMR and ^{13}C-NMR data were collected on a Varian Gemini/2000 400 MHz NMR Spectrometer. High resolution mass spectrometry was performed using electron spray ionization methods.

α-*N*-Fmoc-L-tryptophan 2-amino-5-nitroanilide (1a)

N-methylmorpholine (1.670 mL, 12.19 mmol) was added slowly to a solution of *N*-Fmoc-L-Trp(Boc)-OH (4.000 g, 7.596 mmol) in dry THF (76 mL) at -20°C and stirred under nitrogen protection, followed by the dropwise addition of isobutyl chloroformate (0.990 mL, 7.596 mmol). The reaction was allowed to stir for 20 minutes after which 4-nitro-1,2-phenylenediamine (1.163 g, 7.596 mmol) was added and stirred at -15°C for 2 hours, then room temperature overnight. The reaction mixture was filtered through celite and the filtrate was evaporated to dryness. The residue was dissolved in ethyl acetate and washed consecutively with saturated NH_4Cl, brine, sodium phosphate buffer (0.5 M, pH 7.0), and brine. The combined organic fractions were dried with Na_2SO_4, filtered, and the solvent was evaporated under vacuum. The crude material was purified by flash column chromatography on silica gel (DCM/EtOAc, gradient of 12:1, 10:1, 9:1) to give the desired product **1a** as a yellow solid (68%). ^{1}H-NMR (DMSO) δ 9.48 (s, 1H), 8.05 (d, 2H), 7.87 (d, 1H), 7.89-7.86 (m, 3H), 7.78 (d, 1H), 7.68-7.64 (m, 3H), 7.42-7.23 (m, 6H), 6.76 (d, 1H), 6.44 (s, 1H), 4.54 (q, 1H), 4.26-4.18 (m, 3H), 3.30-3.20 (m, 1H), 3.11-3.04 (m, 1H), 1.58 (s, 9H). ^{13}C-NMR δ 171.6, 156.7, 150.1, 149.6, 144.3, 141.3, 136.0, 135.3, 130.8, 128.2, 127.6, 125.9, 125.0, 124.7, 123.9, 123.0, 122.7, 121.5, 120.7, 120.2, 117.1,

115.3, 114.2, 84.1, 66.5, 55.7, 47.3, 28.3, 27.6. HRMS calcd for $C_{37}H_{35}N_5O_7Na$ [M+Na] 684.2429, found 684.2434.

α-*N*-Fmoc-L-tryptophan 2-amino-5-nitrothioanilide (2a)

Dry THF (690 μL) was added to P_4S_{10} (31.0 mg, 69.6 μmol) and sodium carbonate (7.37 mg, 69.6 μmol) and stirred at room temperature under nitrogen protection for 1 hour, after which the reaction mixture was cooled to 0°C and **1a** (25.6 mg, 36.6 μmol) was added and stirred for 30 minutes. The reaction was then warmed to room temperature and stirred for 2 hours. The solvent was removed under vacuum. The residue was then dissolved in EtOAc/Hexane (2:1) and washed twice with sodium phosphate buffer (0.5 M, pH 7.0). The aqueous wash was back extracted twice with EtOAc/Hexane (2:1). The organics were combined, washed with brine, dried with Na_2SO_4, filtered and solvent was removed under vacuum. Crude material was purified by flash column chromatography on silica gel (DCM/EtOAc, 2:1) to give the desired product **2a** as a yellow solid (79%). ^{1}H-NMR (DMSO) δ 11.41 (s, 1H), 8.20 (d, 1H), 8.07 (d, 1H), 7.97 (d, ½ H), 7.94 (d, ½ H), 7.89 (d, 2H), 7.83 (d, 1H), 7.76 (s, 1H), 7.71-7.68 (m, 3H), 7.42-7.27 (m, 6H), 6.79 (d, 1H), 6.35 (s, 2H), 4.78 (q, 1H), 4.32-4.17 (m, 3H), 3.24-3.16 (m, 1H), 1.62 (s, 9H). ^{13}C-NMR δ 207.4, 156.9, 151.1, 149.7, 144.3, 144.1, 141.3, 135.9, 135.2, 130.8, 128.2, 127.6, 126.0, 125.9, 125.6, 125.3, 125.1, 125.0, 123.0, 122.8, 120.7, 120.3, 116.9, 115.3, 114.5, 84.2, 66.6, 61.7, 47.2, 30.0, 28.4. HRMS calcd for $C_{37}H_{35}N_5O_6SNa$ [M+Na] 700.2200, found 700.2206.

1-(*N*-Fmoc-L-thionotryptophaninyl)-6-benzotriazole (3a)

2a (25.0 mg, 36.9 μmol) was dissolved in a solution of acetic acid/5% water (276 μL) by gentle warming and stirring at 40°C. The reaction mixture was cooled to 0°C and sodium nitrite (3.82 mg, 55.33 μmol) was added in small portions over 5 minutes. After 30 minutes, ice water (1.9 mL) was added. The precipitate was filtered off, washed with ice water, and dried in the lyophilizer overnight to give **3a** (95%). Material was produced in sufficient purity to be directly incorporated into SPPS. ^{1}H-NMR ($CDCl_3$) δ 9.58 (s, 1H), 8.46 (d, 1H), 8.31 (d, 1H), 8.05 (d, 1H), 7.76-7.75 (m, 2H), 7.60-7.18 (m, 10H), 6.65-6.63 (m, 1H), 5.78 (d, 1H), 4.46-4.42 (m, 2H), 4.33-4.29 (m, 1H), 4.20-4.18 (m, 1H), 3.55 (d, ½ H), 3.53 (d, ½ H), 3.29-3.23 (m, 1H), 1.65 (s, 9H). ^{13}C-NMR δ 208.1, 155.7, 149.7, 149.5, 149.1, 143.8, 141.4, 135.4, 131.9, 130.1, 127.9, 127.2, 125.1, 124.9, 123.0, 122.4, 121.6, 120.1, 119.0, 115.5, 114.5, 112.7, 84.1, 67.3, 61.5, 47.3, 32.7. HRMS calcd for $C_{37}H_{32}N_6O_6SNa$ [M+Na] 711.1996, found 711.2002.

α-*N*-Fmoc-L-phenylalanine 2-amino-5-nitroanilide (1b)

N-methylmorpholine (1.670 mL, 12.19 mmol) was added slowly to a solution of *N*-Fmoc-L-Phe-OH (2.943 g, 7.596 mmol) in dry THF (76 mL) at -20°C and stirred under nitrogen protection, followed by the dropwise addition of isobutyl chloroformate (0.990 mL, 7.596 mmol). The reaction was allowed to stir for 20 minutes after which 4-nitro-1,2-phenylenediamine (1.163 g, 7.596 mmol) was added and stirred at -15°C for 2 hours, then room temperature overnight. The reaction was filtered through filter paper (slow)

and the precipitate was collected and dried under vacuum. The crude material **1b** was used directly in the next step.

α-*N*-Fmoc-L-phenylalanine 2-amino-5-nitrothioanilide (2b)

Dry THF (76.5 mL) was added to P_4S_{10} (3.30 g, 7.65 mmol) and sodium carbonate (781 mg, 7.65 mmol) and stirred at room temperature under nitrogen protection for 1 hour, after which the reaction mixture was cooled to 0°C and **1b** (2.14 g, 3.92 mmol) was added and stirred for 30 minutes. The reaction was then warmed to room temperature and stirred for 2 hours. The solvent was removed under vacuum. The residue was then dissolved in EtOAc and washed twice with sodium phosphate buffer (0.5 M, pH 7.0). The aqueous wash was back extracted twice with EtOAc. The organics were combined, washed with brine, dried with Na_2SO_4, filtered and solvent was removed under vacuum. Crude material was purified by flash column chromatography on silica gel (DCM/EtOAc, 12:1) to give the desired product **2b** as a yellow solid (54%). ^{1}H-NMR (DMSO) δ 11.27 (s, 1H), 8.14 (d, 1H), 7.95-7.92 (m, 1H), 7.90 (d, 2H), 7.72 (t, 2H), 7.58 (s, 1H), 7.44-7.25 (m, 10H), 6.75 (d, 1H), 6.20 (s, 2H), 4.70 (q, 1H), 4.31-4.28 (m, 1H), 4.23-4.18 (m, 2H), 3.17-3.06 (m, 2H). ^{13}C-NMR δ 207.3, 170.9, 156.8, 151.1, 144.4, 144.2, 141.3, 137.9, 135.9, 130.1, 128.7, 128.3, 127.7, 127.2, 126.0, 125.9, 125.5, 125.2 ,122.8,120.7,114.5. HRMS calcd for $C_{30}H_{26}N_4O_4SNa$ [M+Na] 561.1567, found 561.1572.

1-(*N*-Fmoc-L-thionophenylalaninyl)-6-benzotriazole (3b)

2b (0.95 g, 1.67 mmol) was dissolved in a solution of acetic acid/5% water (13.2 mL) by gentle warming and stirring at 40°C. The reaction mixture was cooled to 0°C and sodium nitrite (182 mg, 2.65 mmol) was added in small portions over 5 minutes. After 30 minutes, ice water (85 mL) was added. The precipitate was filtered off, washed with ice water, and dried in the lyophilizer overnight to give **3b** (88%). Material was produced in sufficient purity to be directly incorporated into SPPS. ^{1}H-NMR ($CDCl_3$) δ 9.64 (s, 1H), 8.47 (d, 1H), 8.32 (d, 1H), 7.77 (d, 2H), 7.55-7.53 (m, 1H), 7.41-7.39 (m, 1H), 7.34-7.18 (m, 10H), 6.60-6.58 (m, 1H), 5.70 (d, 1H), 4.45-4.33 (m, 3H), 4.21-4.19 (m, 1H), 3.45 (d, ½ H), 3.42 (d, ½ H), 3.16-3.10 (m, 1H). ^{13}C-NMR δ 208.0, 155.6, 149.7, 149.1, 143.7, 141.4, 135.2, 131.9, 129.5, 128.7, 127.9, 127.6, 127.2, 125.2, 122.4, 121.7, 120.2, 112.8, 67.3, 62.5, 47.4, 43.0. HRMS calcd for $C_{30}H_{23}N_5O_4SNa$ [M+Na] 572.1363, found 572.1368.

α-*N*-Fmoc-L-glycine 2-amino-5-nitroanilide (1c)

Protocol identical to the synthesis of α-*N*-Fmoc-L-tryptophan 2-amino-5-nitroanilide **1a**. Crude material **1c** was used directly in next step.

α-*N*-Fmoc-L-glycine 2-amino-5-nitrothioanilide (2c)

Protocol identical to the synthesis of α-*N*-Fmoc-L-tryptophan 2-amino-5-nitrothioanilide **2a**. The crude material was purified by flash column chromatography on silica gel (DCM/EtOAc, 6:1) resulting in desired product **2c** (61%). ^{1}H-NMR (DMSO) δ 11.06 (s,

1H), 7.96 (d, 2H), 7.75 (d, 2H), 7.44-7.32 (m, 4H), 6.85 (d, 1H), 6.55 (s, 2H), 4.35 (d, 2H), 4.03 (m, 1H), 3.39 (s, 1H), 3.35 (s, 2H). ^{13}C-NMR δ 203.2, 157.1, 151.3, 144.4, 141.3, 135.8, 128.2, 127.7, 125.9, 125.6, 125.5, 122.9, 120.7, 114.5, 66.5, 60.4, 52.1, 47.3, 21.4, 14.8. HRMS calcd for $C_{23}H_{21}N_4O_4S$ [M+1] 449.12780, found 449.12835

1-(*N*-Fmoc-L-thionoglycinyl)-6-benzotriazole (3c)

2c (302 mg, 0.69 mmol) was dissolved in a solution of acetic acid/5% water (5.2 mL) by gentle warming and stirring at 40°C. The addition of DMF (2 mL) and MeCN (2mL) along with vigorous stirring was required to completely dissolve the substrate. The reaction mixture was cooled to 0°C and sodium nitrite (71.6 mg, 1.00 mmol) was added in small portions over 5 minutes. After 30 minutes, ice water (1 mL) was added. The precipitate was filtered off, washed with ice water, and dried in the lyophilizer overnight to give **3c** (95%). Material was produced in sufficient purity to be directly incorporated into SPPS. ^{1}H-NMR ($CDCl_3$) δ 9.65 (s, 1H), 8.46 (d, 1H), 8.33 (d, 1H), 7.79 (d, 2H), 7.66 (d, 2H), 7.45-7.33 (m, 4H), 5.22 (d, 1H), 4.51 (d, 2H), 4.30-4.27 (m, 1H), 2.96 (s, 1H), 2.89 (s, 1H). ^{13}C-NMR δ 202.4, 156.5, 149.7, 148.9, 143.8, 141.4, 131.9, 127.9, 127.2, 125.2, 122.4, 121.7, 120.2, 112.6, 107.9, 67.5, 53.1, 47.4, 20.8. HRMS calcd for $C_{23}H_{18}N_5O_4S$ [M+1] 460.10740, found 460.10795.

α-*N*-Fmoc-D-leucine 2-amino-5-nitroanilide (1d)

Protocol identical to the synthesis of α-*N*-Fmoc-L-tryptophan 2-amino-5-nitroanilide **1a**. Crude material **1d** was used directly in the next step. ^{1}H-NMR (DMSO) δ 9.42 (s, 1H),

8.16 (d, 1H), 7.91-7.86 (m, 4H), 7.75-7.71 (m, 3H), 7.43-7.40 (t, 2H), 7.34-7.31 (t, 2H), 6.77 (d, 1H), 6.43 (s, 2H), 4.35-4.20 (m, 4H), 1.75-1.63 (m, 1H), 1.63-1.51 (m, 2H), 0.99-0.86 (m, 6H).

α-*N*-Fmoc-D-leucine 2-amino-5-nitrothioanilide (2d)

Protocol identical to the synthesis of α-*N*-Fmoc-L-phenylalanine 2-amino-5-nitrothioanilide **2b**. The crude material was purified by flash column chromatography on silica gel (DCM/EtOAc, 15:1-9:1) resulting in desired product **2d** (69%). ^{1}H-NMR (DMSO) δ 11.38 (s, 1H), 7.97 (m, 2H), 7.88 (d, 2H), 7.75 (m, 2H), 7.44-7.31 (m, 4H), 6.79 (d, 1H), 6.73 (s, 2H), 4.52-4.24 (m, 3H), 3.32 (s, 1H), 1.76-1.69 (m, 3H), 0.98 (d, 3H), 0.94 (d, 3H). ^{13}C-NMR δ 208.8, 157.1, 151.3, 144.5, 144.2, 141.3, 135.9, 128.3, 127.7, 126.0, 125.9, 125.6, 125.3, 123.0, 120.7, 114.5, 66.5, 60.3, 47.3, 43.5, 25.0, 23.5, 22.6, 21.4, 14.8. HRMS calcd for $C_{27}H_{29}N_4O_4S$ [M+Na] 527.1729, found 527.1729.

1-(*N*-Fmoc-D-thionoleucinyl)-6-benzotriazole (3d)

Protocol identical to 1-(*N*-Fmoc-L-thionotryptophaninyl)-6-benzotriazole **3a**. Product **3d** was produced in sufficient purity (75%) and thus directly incorporated into SPPS. ^{1}H-NMR ($CDCl_3$) δ 9.67 (s, 1H), 8.45 (d, 1H), 8.31 (d, 1H), 7.78 (d, 2H), 7.61 (d, 2H), 7.41-7.32 (m, 4H), 6.31-6.29 (m, 1H), 5.62 (d, 2H), 4.55-4.51 (m, 1H), 4.42-4.37 (m, 1H), 4.24-4.22 (m, 1H), 1.91-1.79 (m, 3H), 1.12 (d, 3H), 0.97 (d, 3H). ^{13}C-NMR δ 210.7, 156.0, 149.7, 149.1, 143.8, 141.5, 132.1, 127.9, 127.2, 125.2, 122.3, 121.6, 120.2, 113.0, 67.1, 60.7, 47.5, 46.1, 25.9, 23.5, 21.5. HRMS calcd for $C_{27}H_{26}N_5O_4S$ [M+1] 516.17000, found 516.17055.

General Methods: Peptide Synthesis and Analysis

Amino acids were purchased from Advanced Chemtech (Louisville, KY) and resins were purchased from Novabiochem (San Diego, CT). Peptide synthesis was carried out on a Tribute Peptide Synthesizer (Protein Technologies, Tucson, AZ). Peptides were centrifuged using a Damon/IEC HN-SII Centrifuge, with the exception of Gramicidin A (and mutant) peptides which were centrifuged using a Beckman Coulter Avanti® J-E Centrifuge. ^{1}H-NMR data for the peptides were taken on a Varian Unity INOVA 500 MHz NMR Spectrometer using a Varian 5 mm Broadband or Varian 5 mm Indirect Detection Probe. Circular dichroism measurements were taken on an Aviv Circular Dichroism Spectrometer, Model 202SF (Aviv Biomedical, Inc., Lakewood, NJ) using a 2 mm quartz cell. Peptide concentrations were determined by measuring absorptions at 280 nm on a Lambda 25 (PerkinElmer, Waltham, MA) in a 10 mm quartz cell. Liposomes were prepared from DOPC provided by Avanti Polar Lipids (Alabaster, AL). All peptides, except for Gramicidin A (and mutants) were purified by high performance liquid chromatography on Waters Prep LC System using a Waters 2489 UV/Visible Detector with a Jupiter 10u C18 300A Column (Waters Corporation, Milford, MA). Molecular masses of Gramicidin A (and mutants) were measured using Waters 2695 Separations Module with the Waters Dual λ Absorbance Detector on a Jupiter 5u C4 300A Column (Waters Corporation, Milford, MA) with a Micromass LCT (UK). Size-exclusion high performance liquid chromatography was performed using Waters e2695 Separations Module with a Waters 2489 UV/Visible Detector and a Styragel® HR 3 (THF) Column (Waters Corporation, Milford, MA).

Preloading Fmoc-Trp-OH onto Wang Resin: Wang Resin [100-200 mesh] (1.0 g, 0.65 mmol) was allowed to swell in DMF for 30-60 minutes. Meanwhile, Fmoc-Trp-OH was dissolved in 10% DMF in DCM (30 mL) and cooled to 0°C after which DIC (0.51 mL, 3.25 mmol) was added dropwise and stirred under nitrogen for twenty minutes. DCM was then removed from the Trp using a vacuum. The reside was then dissolved in minimal volume of DMF and transferred to the swollen resin along with DMAP (7.9 mg, 0.065 mmol) and stirred. After one hour, the DMF was drained and the resin was rinded/swirled with DMF (6 X 5 mL) and finally dried with DCM. The loading capacity was tested using UV/Vis Spectroscopy according to a previously reported method[30].

Synthesis of Trpzip4, GB1, and MW-β-hairpin: Peptides were synthesized using automated solid phase peptide synthesis on a 0.1 mmole scale on Rink Resin SS [75-100 mesh, 1% DVB, substitution: 0.7 mmole/gram]. Five molar equivalents of commercially available amino acids were used for the coupling reactions. The incorporation of unnatural amino acids was accomplished by using five equivalents of the Fmoc-protected amino acid with extended coupling times (2 hours). When applicable, peptides were acetylated using acetic anhydride (10% in DMF, 1 hour, 25°C). The resin was then washed with DMF and dried using DCM. Peptides were cleaved from the dried resin and deprotected with Reagent K (85% trifluoroacetic Acid, 5% phenol, 5% thioanisole, 2.5% water, 2.5% ethanedithiol, 1 hour, 25°C). The resin was then filtered off, and the peptide was precipitated from the filtrate using diethyl ether (25 mL, -78°C). The mixture was centrifuged (8,000 rpm, 15 minutes, 25°C) and the supernatant was discarded. This procedure was repeated 2 times, and finally the peptide was dried under a stream of

nitrogen followed by high vacuum. Crude product was purified by RP-HPLC (CH_3CN/H_2O) upon which purified peptides were subjected to spectroscopic and thermodynamic analysis

Synthesis of Gramicidin A and mutants: Peptides were synthesized using Fmoc strategy via automated solid phase peptide synthesis on a 0.1 mmole scale on Fmoc-Trp-Wang resin. Five molar equivalents of commercially available amino acids were used for the coupling reactions. The incorporation of unnatural amino acids was accomplished by using five equivalents of the Fmoc-protected amino acid with extended coupling time (2 hours). Coupling was monitored using UV/Vis spectroscopy. Incomplete coupling was resolved by capping with acetic anhydride (10% in DMF, 30 min, 25°C). Following capping, the resin was rinsed in DMF and returned to SPPS. *N*-Formyl valine, synthesized according to literature,[27] was introduced under the standard coupling conditions on SPPS. When the synthesis was complete, the resin was dried under vacuum for several hours, after which the peptides were cleaved from the resin with distilled ethanolamine (10% in DMF, 3 mL, 4 hours, 55°C). Upon completion, the reaction mixture was cooled to room temperature and filtered. The resin was rinsed with methanol, followed by dichloromethane and condensed to the original volume of cleavage solution (approx. 3 mL). The peptide was precipitated with Millipore water (approx. 20 mL) and placed on ice for 30 minutes. The mixture was centrifuged (14,000 rmp, 2 hours, 4°C). The supernatant was discarded, and the pellet of peptide was resuspended in a minimal volume of methanol, re-precipitated with water (approx. 10

mL), placed on ice for 30 minutes, centrifuged, and then dried overnight under high vacuum resulting in a white powder. Identity and purity was verified using LC-MS.

Preparation of Liposomes: Liposomes were prepared using 1,2-dioleoyl-sn-glycero-3-phosphocholine. DOPC (final concentration 50 mM,) was dissolved in chloroform and thoroughly mixed. Chloroform was removed under vacuum and allowed to dry overnight. Lipids were then hydrated with buffer (10 mM NaP_i, 100 mM NaCl, 10 uM HPTS, pH 7.0). Full encapsulation and vesicle formation was ensured by performing 20 freeze-thaw cycles (-78°C, 80°C), followed by extrusion (25 times) using an extruder with a 100 nm filter (Avanti Polar Lipids) to ensure uniform size. LUVs were then purified via gel filtration using a UPC-900 system with a sephacryl S-500 column (General Electric, Piscataway, NJ), eluted with 10 mM NaP_i, pH 7.0. Purity of the eluent was monitored by UV/Vis. The resulting purified liposome stock was 10 mM.

Leakage Assay using Fluorescence: To a 1.0 cm quartz cuvette with stir bar was added sodium phosphate (10 mM, pH 7.0, 1.640 mL), liposomes prepared according to procedure described above (10 mM, 100 μL), and cesium chloride solution prepared in NaP_i buffer (1M, 200 uL). The emission of HPTS ($\lambda_{emission}$ = 510 nm) was monitored at $\lambda_{excitation}$ = 460 nm. After 100 seconds, NaOH (0.5 M, 10 μL) was titrated into the cuvette. After signal reached a plateau (approx 200 s), gA sample (50 μM in THF, 50 μL) and continued to stir. At 500 seconds, Triton X-100 (5% in NaP_i, pH 7.5, 40 μL) was titrated into the cuvette. Data was collected for 600 seconds.

REFERENCES

References

1. Leader, B.; Baca, Q. J.; Golan, D. E., Protein therapeutics: a summary and pharmacological classification. *Nat Rev Drug Discov* **2008,** 7, (1), 21-39.
2. Wikipedia. http://en.wikipedia.org/wiki/ (March 24, 2009),
3. De Smet, K.; Contreras, R., Human antimicrobial peptides: defensins, cathelicidins and histatins. *Biotechnol Lett* **2005,** 27, (18), 1337-47.
4. Dashper, S. G.; Liu, S. W.; Reynolds, E. C., Antimicrobial peptides and their potential as oral therapeutic agents. *International Journal of Peptide Research and Therapeutics* **2007,** 13, (4), 505-516.
5. Brogden, K. A., Antimicrobial peptides: pore formers or metabolic inhibitors in bacteria? *Nat Rev Microbiol* **2005,** 3, (3), 238-50.
6. Nelson, D. L. C., Michael M., *Principles of Biochemistry*. Fourth Edition ed.; W. H. Freeman and Company: New York, 2005.
7. Jelinek, R.; Kolusheva, S., Membrane interactions of host-defense peptides studied in model systems. *Curr Protein Pept Sci* **2005,** 6, (1), 103-14.
8. Jeffrey, G. A. S., W., *Hydrogen Bonding in Biological Structures*. Springer-Verlag: Berlin, 1994.
9. Fu, Y.; Bieschke, J.; Kelly, J. W., E-olefin dipeptide isostere incorporation into a polypeptide backbone enables hydrogen bond perturbation: probing the requirements for Alzheimer's amyloidogenesis. *J Am Chem Soc* **2005,** 127, (44), 15366-7.
10. Sammes, P. G. H., Michael M.; Kennewell, Peter D.; Taylor, John B., On Double Bond Isosteres of the Peptide Bond; an Enkephalin Analogue. *J.C.S. Chem. Comm.* **1980**, 234-235.
11. Sammes, P. G. M., Nicholas J.; Kennewell, Peter D.; Westwood, Robert, On the Double Bond Isostere of the Peptide Bond: Preparation of Modified Di- and Tri-peptides incorporating Proline and Alanine Analogues. *J. Chem. Soc. Perkin Trans.* **1985,** 1.
12. Jenkins, C. L.; Vasbinder, M. M.; Miller, S. J.; Raines, R. T., Peptide bond isosteres: ester or (E)-alkene in the backbone of the collagen triple helix. *Org Lett* **2005,** 7, (13), 2619-22.
13. Miwa, J. H.; Pallivathucal, L.; Gowda, S.; Lee, K. E., Conformational stability of helical peptides containing a thioamide linkage. *Org Lett* **2002,** 4, (26), 4655-7.
14. Miwa, J. H.; Patel, A. K.; Vivatrat, N.; Popek, S. M.; Meyer, A. M., Compatibility of the thioamide functional group with beta-sheet secondary structure: incorporation of a thioamide linkage into a beta-hairpin peptide. *Org Lett* **2001,** 3, (21), 3373-5.
15. Shalaby, M. A.; Grote, C. W.; Rapoport, H., Thiopeptide Synthesis. alpha-Amino Thionoacid Derivatives of Nitrobenzotriazole as Thioacylating Agents. *J Org Chem* **1996,** 61, (25), 9045-9048.
16. Horne, W. S.; Gellman, S. H., Foldamers with heterogeneous backbones. *Acc Chem Res* **2008,** 41, (10), 1399-408.

17. Zhang, Z. L.; Pascal, S. M.; Cross, T. A., A Conformational Rearrangement in Gramicidin-a - from a Double-Stranded Left-Handed to a Single-Stranded Right-Handed Helix. *Biochemistry* **1992,** 31, (37), 8822-8828.
18. Blanco, F. J.; Rivas, G.; Serrano, L., A Short Linear Peptide That Folds into a Native Stable Beta-Hairpin in Aqueous-Solution. *Nature Structural Biology* **1994,** 1, (9), 584-590.
19. Cochran, A. G.; Skelton, N. J.; Starovasnik, M. A., Tryptophan zippers: Stable, monomeric beta-hairpins. *Proceedings of the National Academy of Sciences of the United States of America* **2001,** 98, (10), 5578-5583.
20. Tatko, C. D.; Waters, M. L., Selective aromatic interactions in beta-hairpin peptides. *J Am Chem Soc* **2002,** 124, (32), 9372-3.
21. Tatko, C. D.; Waters, M. L., Effect of halogenation on edge-face aromatic interactions in a beta-hairpin peptide: Enhanced affinity with Iodo-substituents. *Organic Letters* **2004,** 6, (22), 3969-3972.
22. Tatko, C. D.; Waters, M. L., The geometry and efficacy of cation-pi interactions in a diagonal position of a designed beta-hairpin. *Protein Sci* **2003,** 12, (11), 2443-52.
23. Syud, F. A.; Stanger, H. E.; Gellman, S. H., Interstrand side chain--side chain interactions in a designed beta-hairpin: significance of both lateral and diagonal pairings. *J Am Chem Soc* **2001,** 123, (36), 8667-77.
24. Veatch, W. R.; Blout, E. R., Aggregation of Gramicidin-a in Solution. *Biochemistry* **1974,** 13, (26), 5257-5264.
25. Abdul-Manan, N.; Hinton, J. F., Conformation states of gramicidin A along the pathway to the formation of channels in model membranes determined by 2D NMR and circular dichroism spectroscopy. *Biochemistry* **1994,** 33, (22), 6773-83.
26. Greathouse, D. V.; Hinton, J. F.; Kim, K. S.; Koeppe, R. E., Gramicidin-a Short-Chain Phospholipid Dispersions - Chain-Length Dependence of Gramicidin Conformation and Lipid Organization. *Biochemistry* **1994,** 33, (14), 4291-4299.
27. Greathouse, D. V.; Koeppe, R. E., 2nd; Providence, L. L.; Shobana, S.; Andersen, O. S., Design and characterization of gramicidin channels. *Methods Enzymol* **1999,** 294, 525-50.
28. Salom, D.; Perez-Paya, E.; Pascal, J.; Abad, C., Environment- and sequence-dependent modulation of the double-stranded to single-stranded conformational transition of gramicidin A in membranes. *Biochemistry* **1998,** 37, (40), 14279-14291.
29. Sun, H.; Greathouse, D. V.; Andersen, O. S.; Koeppe, R. E., The preference of tryptophan for membrane interfaces - Insights from n-methylation of tryptophans in gramicidin channels. *Journal of Biological Chemistry* **2008,** 283, (32), 22233-22243.
30. *Novabiochem Catalog*. EMD Biosciences, Inc. : San Diego, CA, 2006.
31. Sidorov, V.; Kotch, F. W.; Abdrakhmanova, G.; Mizani, R.; Fettinger, J. C.; Davis, J. T., Ion channel formation from a calix[4]arene amide that binds HCl. *Journal of the American Chemical Society* **2002,** 124, (10), 2267-2278.